STAR OCCULTATION MEASUREMENTS

AS AN AID TO NAVIGATION IN

CIS-LUNAR SPACE

by

ROY VINCENT KEENAN

S.B., University of Nebraska
(1957)

JOHN DONALD REGENHARDT

S.B., United States Naval Academy
(1957)

SUBMITTED IN PARTIAL FULFILLMENT

OF THE REQUIREMENTS FOR THE

DEGREE OF MASTER OF SCIENCE

at the

MASSACHUSETTS INSTITUTE OF TECHNOLOGY

June, 1962

Signature of Authors_____

Department of Aeronautics
and Astronautics, June 1961

Certified by_____ _____
Thesis Supervisor

Accepted by_____
Chairman, Departmental
Graduate Committee

STAR OCCULTATION MEASUREMENTS
AS AN AID TO NAVIGATION IN
CIS-LUNAR SPACE

by

Roy V. Keenan
John D. Regenhardt

Submitted to the Department of Aeronautics and
Astronautics on May 19, 1962 in partial fulfillment
of the requirements for the degree of Master of Science.

ABSTRACT

The time measurement of star occultations is one of several
modes of obtaining navigation data in cis-lunar space. Using
statistical methods of optimization of data, the feasibility
of navigation using the measurement of star occultations as
a method in itself and in combination with angle measure-
ments is investigated using digital computation techniques.
The real star field is approximated by a statistical star back-
ground for the purpose of this study. An "average occultation
frequency" is calculated based on a reference trajectory and
the statistical star background. The occurrence or non-
occurrence of occultations along the trajectory is determined
by a random number operation which utilizes the "average
occultation frequency". The measurements obtained are
introduced into a navigation routine which simulates the
circumlunar voyage. The results indicate that navigation
based on occultation measurements alone is not practical.
However, when occultation measurements are used in conjunction
with angle measurements, it is shown that the total velocity
correction required is reduced and other navigational
parameters are similarly reduced. This study indicates that
further investigation using actual star data would be
appropriate.

Thesis Supervisor: Walter Wrigley, Sc.D.

Title: Professor of Instrumentation and
Astronautics

Thesis Supervisor: Richard H. Battin, Ph.D.

Title: Lecturer in Aeronautics and
Astronautics

ACKNOWLEDGEMENTS

This report was prepared under the auspices of
DSR Project 55-191, sponsored by the Manned Spacecraft
Center of the National Aeronautics and Space Administration
through Contract NAS 9-153.

The publication of this report does not constitute
approval by the National Aeronautics and Space Administration
of the findings or conclusions contained therein. It is
published only for the exchange and stimulation of ideas.

TABLE OF CONTENTS

CHAPTER I

INTRODUCTION

As seen from a vehicle traveling in earth-moon
space, stars will disappear behind the earth or the moon
due to the relative movement of those bodies with
respect to the vehicle. In a like manner stars will
appear from behind the earth and the moon. The word
occultation will be used in this study to include both
phenomena, although in the strict sense this word
applies only to the disappearance of one celestial body
due to the intervention of a second celestial body.

By noting the time that an occultation of a known
star takes place, an astronaut may gain information
about the vehicle's position and velocity. The same
kind of information may be gained by other types of
measurements.[1] One family of measurements available
is comprised entirely of angular measurements. In-
cluded in this category are measurements of the angle
between the moon horizon and the earth horizon, the moon
horizon and a star, an earth landmark and a star and
other obvious combinations. Also included in this
family is the measurement of the apparent diameter of

either the earth or the moon. A second family is comprised entirely of measurements utilizing electromagnetic radiation.

All of the angular measurements require some sort of space sextant and possibly some maneuvering of the space vehicle. The electromagnetic techniques would also involve additional equipment and perhaps some maneuvering. In contrast the occultation measurements would require no equipment other than a precision time source which would already be included in any self contained navigation system. Assuming that omnidirectional vision would be provided by periscopes, occultation measurements would require no maneuvering of the space vehicle. The observer would simply record the instant of occultation. Thus the measurement would cost nothing in the way of propellant to maneuver the vehicle and would require no extra equipment in the vehicle. There is one other important difference between occultation measurements and the other measurements mentioned. The angular measurements and the electromagnetic measurements are available over some continuous time interval, whereas occultations are discrete events.

To be of real use occultations must meet two criteria. They must occur frequently enough to provide more than sporadic information, and the information they

provide must be of usable quality. Both of these factors will be investigated in the work that follows.

Several possibilities for the use of occultation measurements in space navigation present themselves. Perhaps a successful voyage could be made using only occultation data for navigation. More probably occultation measurements could be used to supplement other techniques. In connection with the latter idea, it is interesting to note that angular measurements are more easily made from an illuminated horizon while occultations are most accurately observed when they take place at a non-illuminated portion of the occulting body. Thus it appears that angular measurements and occultation measurements complement one another. Finally it is possible that occultation measurements could provide an emergency navigation technique in the event of failure of a more sophisticated system.

The purpose of this thesis is to study the usefulness of star occultation data for navigational purposes during a circum-lunar voyage. There are several logical steps that must be taken before any conclusions can be drawn. First, it must be established that occultations occur frequently enough to be useful. Here, the authors have drawn heavily from an unpublished study on star

occultation frequency by Dr. J. H. Laning Jr.[2] This
study indicated that occultations do occur frequently
enough to warrant investigation into their useful-
ness as an aid to navigation. This result motivated
the work that is the main body of the present study.

A control program, utilizing existing subroutines
and an existing trajectory, was written to simulate a
circum-lunar flight. Options were written into the
control program so that the use of two navigational
modes could be simulated. In one case the navigation
is based entirely on occultation measurements. In
the second case navigation is based on a combination of
angle and occultation measurements.

It should be noted here that the entire study is
a statistical simulation of the actual problem. The
frequency with which occultations would occur is com-
puted on the basis of a statistical star background.
A random number process based on this frequency
determines whether an occultation actually occurs, and
a similar process determines where on the body the
occultation takes place.

A simulated flight is begun by estimating injection
errors in position and velocity. These initial errors
are chosen on the basis of a statistical knowledge of
the launch guidance capabilities. Upon completion of

a simulated flight, the effectiveness of the navigation
technique employed can be evaluated on the basis of the
resulting errors in position and velocity at the target,
the accuracy with which these errors are known and the
required velocity corrections.

CHAPTER 2

NAVIGATION THEORY

2.1 Introduction

For the past several years there has been consider-
able thought and effort devoted to the ways and means
of midcourse navigation of both manned and un-manned
space flight vehicles. This study will concern itself
with the work of Dr. R. H. Battin and his method for
optimum utilization of space navigation data.[1]

For the purposes of clarity and cohesiveness a
summary of Dr. Battin's approach to this problem of
optimum utilization of navigation data will be included
here, but the reader is directed to the above reference
for a more comprehensive study.

This summary will be further limited to the applica-
tion of Dr. Battin's work to star occultation measurement
data in earth-moon space in accordance with the area of
this study and with the fact that other measurement modes
are utilized in an entirely analogous manner.

2.2 General

Star occultation navigation is founded on small per-
turbation theory in which only small deviations from the
referenced times of occultation and the corresponding
small deviations in position and velocity from a reference
trajectory are utilized. Data are obtained by an astro-
naut using a timer device to obtain the time difference
between the actual and referenced times of an occultation,
where an on-board clock will serve as a time reference.
These data will be processed by an on-board computer and
will provide the calculations for any small changes in
the vehicle velocity.

Problems to be solved by using this method of
statistical optimization of star occultation data are:
(1) definition and derivation of the optimum linear
operations for processing the star occultation data in
a manner consistent with the mission objectives; (2)
optimization of the number of corrective maneuveurs re-
quired in terms of mission accuracy; and (3) expression
of the mean-squared velocity correction directly in terms
of the errors associated with initial orbital injection,
star occultation measurements and establishment of the
desired velocity corrections.

It will be assumed throughout this study that the
cross-correlation effects of random measurement errors
is negligible and will therefore be ignored. This

assumption is not true in general but was utilized here for the sake of convenience. Also, launch guidance is not considered so that the guidance problem is confined to the time between injection into and return from a trans-lunar orbit.

Errors arising from lunar orbit injection will be considered small and the corresponding deviations in position will be detected and corrected in the normal course of the star occultation navigation program. Navigationally the outbound and return portions of the trip are basically the same.

Star occultation measurements and velocity corrections will be made at specific points along a specified trajectory, where the time interval and selection of these points is arbitrary with consideration being given to proximity of the vehicle to the target body. That is, the nearer the vehicle is to the reference body, the smaller the integration interval of the equations of motion should be for greater accuracy of trajectory determination. The time limits of these intervals define the location of decision points along the trajectory. For an actual mission the decision points will be those pre-calculated reference times of desired real star occultations. The trajectory is based on a three-dimensional model of the solar system.

In the star occultation mode one of two events can occur at each decision point: (1) either a velocity correction is implemented; or (2) an occultation measurement is initiated if available. This procedure differs from that when using angular measurements only in that it costs nothing but a few seconds of the astronaut's time to make an occultation measurement so that for the sake of better reduction of data uncertainties the occultation measurement should be made at every available opportunity.

Notation conventions utilized are as follows: (1) a column vector of any dimension is represented by an underscored letter with the absolute value identified by omitting the underscore; (2) matrices are denoted by capital letters; (3) the transpose of a vector or a matrix will be denoted by a superscript T; (4) the scalar product of two vectors a and b will be written as $a^T b$; and (5) the average value of any quantity will be indicated by an overscore.

2.3 The Star Occultation Measurement

The reference time T is defined as that time when a predetermined occultation should occur. At this reference time T for an occultation measurement there exists a reference position vector $\underline{r}$ for the vehicle, and it is assumed that we know the exact position and velocity of the earth

and moon at time T. Time T will correspond to those times establishing decision points along the reference trajectory.

If a position deviation $\delta\underline{r}$ exists, then a specified occultation will not occur at the reference time T so that a time increment $\delta\tau$ is defined as that interval between the referenced and actual occultation times. $\delta\tau$ can be an interval either before or after the reference time T since the probabilities of an occultation occurring before or after the reference time are the same.

It is assumed that there is no clock error present in these measurements and calculations since clocks are currently available with accuracies such that the resultant navigation errors induced in a typical sixty-hour lunar mission is negligible.

To obtain the deviation in time $\delta\tau$ with respect to the position deviation $\delta\underline{r}$ of the vehicle from its reference position, let the relative positions of the sun, occulting body and vehicle be as shown in Fig. 2.1. Let $\underline{r}$ be the vector from the sun to the vehicle S_0 and $\underline{z}$ the vector from S_0 to the center of the occulting body OB. The unit vector $\underline{n}$ is in the direction of the star to be occulted while $\underline{m}$ is the unit vector corresponding to $\underline{z}$. ρ is a unit vector associated with the vector $\underline{x}$ defined as normal to $\underline{m}$ and in the plane of occultation defined by $\underline{m}$ and $\underline{n}$. As shown, γ is the angle between the vehicle-star and the

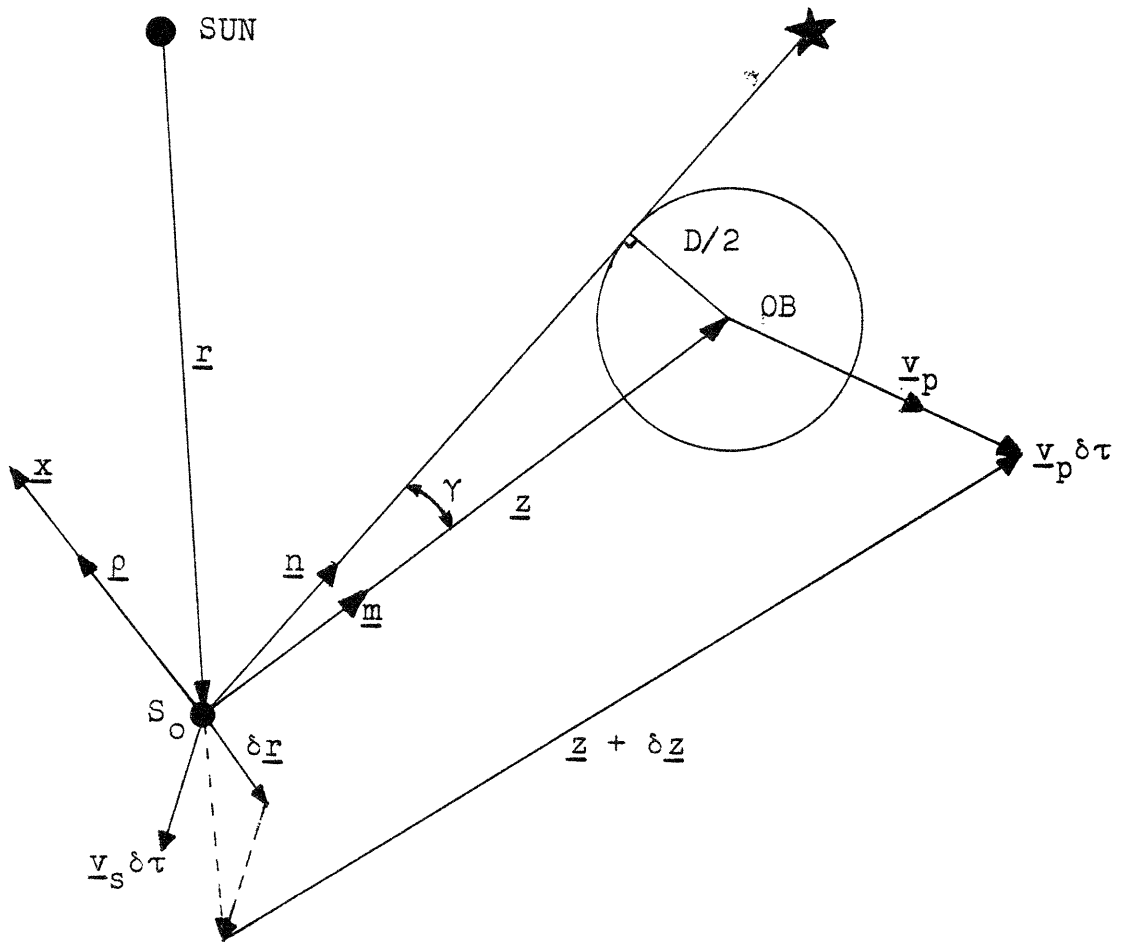vehicle-occulting body center lines.

FIG. 2.1   Star occultation geometry

Factors affecting the relationship between $\delta\tau$ and $\delta\underline{r}$ are (1) motion of the occulting body during the interval $\delta\tau$; (2) the initial displacement $\delta\underline{r}$ of the vehicle position with respect to S_0 at the time T when the occultation should occur; and (3) the vector distance $\underline{v}_s\delta\tau$ traveled by the vehicle with velocity vector $\underline{v}_s$ from the start to finish of the occultation measurement.

At the instant of occultation we have

$$\underline{n}\cdot\underline{z} = z \cos \gamma \qquad (2.2)$$

where

$$z^2 = \underline{z}\cdot\underline{z} \qquad (2.3)$$

Treating changes as first order differentials there results

$$\underline{n}\cdot\delta\underline{z} = \cos \gamma \, \delta z - z \sin \gamma \, \delta\gamma$$
$$= \cos \gamma \, \underline{m}\cdot\delta\underline{z} - z \sin \gamma \, \delta\gamma \qquad (2.4)$$

where

$$\delta z = \underline{m}\cdot\delta\underline{z} \qquad (2.5)$$

The angle γ is also defined by the relation

$$\sin \gamma = \frac{D}{2z} \qquad (2.6)$$

Again taking first order differentials to compute the

angle deviation $\delta\gamma$, there results

$$2 \sin \gamma \, \delta z + 2z \cos \gamma \, \delta\gamma = 0 \qquad (2.7)$$

from which

$$\delta\gamma = - \frac{\sin \gamma \, \delta z}{z \cos \gamma}$$

$$= - \frac{D}{2z^2 \cos \gamma} \, \delta z \qquad (2.8)$$

$$= - \frac{D}{2z^2 \cos \gamma} \, \underline{m} \cdot \delta\underline{z}$$

with the aid of Eq. (2.5).

With $\underline{v}_p$ and $\underline{v}_s$ defining the velocity vectors of the occulting body and vehicle respectively and $\underline{v}_r$ defining the velocity of the vehicle with respect to the occulting body, we have

$$\underline{v}_s = \underline{v}_r + \underline{v}_p \qquad (2.9)$$

From Fig. 2.1 summing vectors

$$\underline{z} + \delta\underline{z} - \underline{v}_p\delta\tau - \underline{z} + \delta\underline{r} + \underline{v}_s\delta t = 0 \qquad (2.10)$$

from which

$$\delta\underline{z} = (\underline{v}_p - \underline{v}_s)\delta\tau - \delta\underline{r}$$

$$= -\underline{v}_r\delta\tau - \delta\underline{r} \qquad (2.11)$$

The vector $\underline{x}$ normal to the unit vector $\underline{m}$ is defined as

$$
\begin{aligned}
\underline{x} &= (\underline{m} \times \underline{n}) \times \underline{m} \\
&= \underline{n}(\underline{m}\cdot\underline{m}) - \underline{m}(\underline{n}\cdot\underline{m}) \\
&= \underline{n} - \underline{m}(\underline{n}\cdot\underline{m}) \\
&= \underline{n} - \cos\gamma\ \underline{m}
\end{aligned}
\tag{2.12}
$$

with magnitude

$$
\begin{aligned}
x &= \sqrt{1 - \cos^2\gamma} \\
&= |\sin\gamma|
\end{aligned}
\tag{2.13}
$$

The unit vector corresponding to $\underline{x}$ is defined as

$$
\begin{aligned}
\underline{\rho} &= \frac{\underline{x}}{x} \\
&= \frac{\underline{n} - \cos\gamma\ \underline{m}}{|\sin\gamma|}
\end{aligned}
\tag{2.14}
$$

using Eqs. (2.12) and (2.13).

Solving Eq. (2.4) for the angular deviation $\delta\gamma$ and using Eqs. (2.8) and (2.14), we have

$$
\begin{aligned}
\delta\gamma &= \frac{(\cos\gamma\ \underline{m} - \underline{n})\cdot\delta\underline{z}}{z\sin\gamma} \\
&= -\frac{1}{z}\underline{\rho}\cdot\delta\underline{z} \\
&= -\frac{D\ \underline{m}\cdot\delta\underline{z}}{2z^2\cos\gamma}
\end{aligned}
\tag{2.15}
$$

Eqs. (2.6) and (2.15) then give us

$$\frac{1}{z} \underline{\rho} \cdot \delta \underline{z} = \frac{D \, \underline{m} \cdot \delta \underline{z}}{2z^2 \cos \gamma}$$

(2.16)

$$= \frac{\tan \gamma}{z} \, \underline{m} \cdot \delta \underline{z}$$

Finally, using Eqs. (2.11) and (2.16) there results

$$\frac{1}{z} \underline{\rho} \cdot (-\delta \underline{r} - \underline{v}_r \delta \tau) = \frac{\tan \gamma}{2} \, \underline{m} \cdot (-\delta \underline{r} - \underline{v}_r \delta \tau)$$

(2.17)

and solving for $\delta \tau$, we have

$$\delta \tau = - \frac{(\underline{\rho} - \tan \gamma \, \underline{m})}{(\underline{\rho} - \tan \gamma \, \underline{m}) \cdot \underline{v}_r} \cdot \delta \underline{r}$$

(2.18)

where the vector $\underline{h}$ is defined as

$$\underline{h} = - \frac{\underline{\rho} - \tan \gamma \, \underline{m}}{(\underline{\rho} - \tan \gamma \, \underline{m}) \cdot \underline{v}_r}$$

(2.19)

enabling us to rewrite Eq. (2.18) as

$$\delta \tau = \underline{h} \cdot \delta \underline{r}$$

$$= h^T \delta \underline{r}$$

(2.20)

Therefore, the vector $\underline{h}$ is dependent upon the geometrical configuration of the vehicle and occulting body combination with respect to the star background on the celestial sphere at the time of measurement.

2.4 Correlation of Deviation Vectors

To relate the results of measurements at times T_n and T_{n+1} a six-dimensional deviation vector $\delta \underline{x}_n$ is introduced and is defined as

$$\delta \underline{x}_n = \left\| \begin{array}{c} \delta \underline{r}_n \\ \delta \underline{v}_n \end{array} \right\|$$

$$= \left\{ \begin{array}{c} \delta r_{1n} \\ \delta r_{2n} \\ \delta r_{3n} \\ \delta v_{1n} \\ \delta v_{2n} \\ \delta v_{3n} \end{array} \right\} \qquad (2.21)$$

where $\delta \underline{r}_n$ is the position deviation vector from the reference path, $\delta \underline{v}_n$ is the velocity deviation vector from the reference value and $\delta \underline{x}_n$ defines the "state" of the vehicle dynamics at time T_n.

$\delta \underline{x}$ at times T_n and T_{n+1} respectively is related by a "transition" matrix such that

$$\delta \underline{x}_n = \Phi_{n,n-1} \; \delta \underline{x}_{n-1} \qquad (2.22)$$

and

$$\delta \underline{x}_{n+1} = \Phi_{n+1,n} \; \delta \underline{x}_n \qquad (2.23)$$

from which

$$\delta \underline{x}_n = \Phi_{n+1,n} \; \delta \underline{x}_{n+1} \qquad (2.24)$$

By defining the rectangular matrix K as

$$K = \left\| \begin{matrix} I \\ 0 \end{matrix} \right\| \qquad (2.25)$$

where I and O represent respectively the three dimensional identity and zero matrices, the position deviation vector $\delta \underline{r}_n$ can be related to $\delta \underline{x}_n$ as

$$\delta \underline{r}_n = \begin{Bmatrix} \delta r_{1n} \\ \delta r_{2n} \\ \delta r_{3n} \end{Bmatrix}$$

$$= \begin{pmatrix} 1 & 0 & 0 & 0 & 0 & 0 \\ 0 & 1 & 0 & 0 & 0 & 0 \\ 0 & 0 & 1 & 0 & 0 & 0 \end{pmatrix} \begin{Bmatrix} \delta r_{1n} \\ \delta r_{2n} \\ \delta r_{3n} \\ \delta v_{1n} \\ \delta v_{2n} \\ \delta v_{3n} \end{Bmatrix} \quad (2.26)$$

$$= K^T \; \delta \underline{x}_n$$

where K^T and $\delta \underline{x}_n$ derive from Eqs. (2.21) and (2.25).

Eqs. (2.24) and (2.26) enable us to rewrite Eq. (2.20) as

$$
\begin{aligned}
\delta \tau_n &= \underline{h}_n \cdot \delta \underline{r}_n \\
&= \underline{h}_n^T \; \delta \underline{r}_n \\
&= \underline{h}_n^T \; K^T \; \delta \underline{x}_n \\
&= \underline{h}_n^T \; K^T \; \Phi_{n+1,n}^{-1} \; \delta \underline{x}_{n+1}
\end{aligned}
\qquad (2.27)
$$

which now relates the effect at time T_{n-1} of an occulta-
tion measurement at time T_n. The vector $\underline{h}_n^T K^T \Phi_{n+1,n}^{-1}$ of
Eq. (2.27) may be rewritten as $\Phi_{n+1,n}^{T-1} K\underline{h}_n$ and each
occultation measurement will yield one component of this
six dimensional deviation vector so that if six occulta-
tions were recorded and no two components were parallel,
the deviation vector could be obtained.

2.5 The Statistical Parameters

Combining additional observations with linear least
squares estimation techniques of analysis, it is possible
to arrive at a more accurate estimate of position and
velocity; and as an added benefit, avoid inverting sixth
order matrices as would be required for a solution above.

In order to explore this technique, several quantities
must be defined. They are (1) the measured deviation in
time $\widetilde{\delta\tau}$; (2) the true deviation in time $\delta\tau$; (3) the
associated error in the occultation measurement α_n which
will be regarded as a random variable; (4) the predicted
value of the position deviation vector $\delta\hat{\underline{r}}_n$; (5) the
actual position deviation vector $\delta\underline{r}_n$; (6) the error in
the position prediction vector $\underline{\varepsilon}_n$; (7) the predicted devia-
tion in velocity $\delta\hat{\underline{v}}_n$; (8) the true velocity deviation $\delta\underline{v}_n$;

and (9) the error in the velocity prediction $\underline{\delta}_n$.

These definitions combine to form the expressions

$$\delta\tilde{\tau}_n = \delta\tau_n + \alpha_n \tag{2.28}$$

$$\delta\hat{\underline{r}}_n = \delta\underline{r}_n + \underline{\varepsilon}_n \tag{2.29}$$

and

$$\delta\hat{\underline{v}}_n = \delta\underline{v}_n + \underline{\delta}_n \tag{2.30}$$

where α_n, $\underline{\varepsilon}_n$ and $\underline{\delta}_n$ are all considered to be random variables. For example, the average value of α_n is $\overline{\alpha_n}$ and the variance is

$$\sigma_n^2 = \overline{\alpha_n^2} - \overline{\alpha_n}^2 \tag{2.31}$$

In a manner analogous to Eqs. (2.28) through (2.30), the optimal linear estimate of $\delta\underline{x}_n$ denoted by $\delta\hat{\underline{x}}_n$ can be written as

$$\delta\hat{\underline{x}}_n = \delta\underline{x}_n + \underline{e}_n \tag{2.32}$$

where $\underline{e}_n$ is the associated six-dimensional estimation error vector defined as

$$\underline{e}_n = \left\|\begin{matrix} \underline{\varepsilon}_n \\ \underline{\delta}_n \end{matrix}\right\| \tag{2.33}$$

$\underline{\varepsilon}_n$ and $\underline{\delta}_n$ are respectively the position and velocity estimation errors as defined in Eqs. (2.29) and (2.30)

The optimal linear estimate $\delta\hat{\underline{x}}_n$ can be updated by a simple recursive formula (cf. Section 2.6). The correlation matrix of the estimation error can be defined as

$$E_n = \overline{\underline{e}_n \underline{e}_n^T}$$

$$= \left\| \begin{matrix} \underline{\varepsilon}_n \\ \underline{\delta}_n \end{matrix} \right\| \; \left\| \begin{matrix} \underline{\varepsilon}_n^T & \underline{\delta}_n^T \end{matrix} \right\|$$

$$= \left\| \begin{matrix} \overline{\underline{\varepsilon}_n \underline{\varepsilon}_n^T} & \overline{\underline{\varepsilon}_n \underline{\delta}_n^T} \\ \overline{\underline{\delta}_n \underline{\varepsilon}_n^T} & \overline{\underline{\delta}_n \underline{\delta}_n} \end{matrix} \right\| \qquad (2.34)$$

$$= \left\| \begin{matrix} E_n^{(1)} & E_n^{(2)} \\ E_n^{(3)} & E_n^{(4)} \end{matrix} \right\|$$

The quantity $\delta\hat{\underline{x}}_n'$ defines an estimate simply extrapolated from a previous estimate as opposed to the estimate $\delta\hat{\underline{x}}_n$ obtained by incorporating an observation at time t_n. Therefore, using the "transition" matrix, $\delta\hat{\underline{x}}_n'$ is defined as

$$\delta\hat{\underline{x}}' = \Phi_{n,n-1} \; \delta\hat{\underline{x}}_{n-1} \qquad (2.35)$$

where

$$\delta\hat{\underline{x}}_{n-1} = \delta\underline{x}_{n-1} + \underline{e}_{n-1} \qquad (2.36)$$

from Eq. (2.32). Combining Eqs. (2.35) and (2.36), we have

$$\delta \hat{\underline{x}}'_n = \Phi_{n,n-1} \, \delta \underline{x}_{n-1} + \Phi_{n,n-1} \, \underline{e}_{n-1} \qquad (2.37)$$

Defining an extrapolated error vector as

$$\underline{e}'_n = \Phi_{n,n-1} \, \underline{e}_{n-1} \qquad (2.38)$$

and using Eq. (2.22), Eq. (2.37) can be rewritten as

$$\delta \hat{\underline{x}}' = \delta \underline{x}_n + \underline{e}'_n \qquad (2.39)$$

The associated extrapolated correlation matrix is defined as

$$E'_n = \overline{\underline{e}'_n \underline{e}'^T_n} \qquad (2.40)$$

Using Eq. (2.38) and its transpose, this can be rewritten as

$$\begin{aligned} E'_n &= \Phi_{n,n-1} \, \overline{\underline{e}_{n-1} \underline{e}^T_{n-1}} \, \Phi^T_{n,n-1} \\ &= \Phi_{n,n-1} \, E_{n-1} \, \Phi^T_{n,n-1} \end{aligned} \qquad (2.41)$$

where

$$E_{n-1} = \overline{\underline{e}_{n-1} \underline{e}^T_{n-1}} \qquad (2.42)$$

from Eq. (2.34).

An estimate of the deviation in the occultation time $\delta\tau$ to be measured at time T_n may be obtained from the extrapolated estimate of $\delta\hat{\underline{x}}_{n-1}$ giving us

$$\delta\hat{\tau}_n' = \underline{h}_n^T K^T \delta\hat{\underline{x}}_n' \qquad (2.43)$$

This relation, when compared to the measured deviation $\delta\tilde{\tau}_n$, is used in arriving at a revised extimate of $\delta\underline{x}_n$.

2.6 Navigation and Guidance Equations

Time t_L corresponds to time of completion of launch and the associated correlation matrix

$$E_0 = E(t_L) \qquad (2.44)$$

is specified initially from a statistical knowledge of injection guidance errors. The initial estimate of position and velocity deviation

$$\delta\hat{\underline{x}}_0 = \delta\hat{\underline{x}}(t_L) \qquad (2.45)$$

is zero since the best unbiased estimate in the absence of any observation is that the vehicle is on course.

A revised estimate $\delta\hat{\underline{x}}(t)$ of the deviation vector $\delta\underline{x}(t)$ is made at each decision point---the form of the revision dependent upon the nature of the decision of which there are two possibilities: (1) a measurement; or

(2) a velocity correction; so that $\delta\hat{\underline{x}}_n$ may be written as

$$
\delta\hat{\underline{x}}_n = \begin{cases} \delta\hat{\underline{x}}_n' + a_n^{-1} E_n' \, K\underline{h}_n \, (\delta\tilde{\tau}_n - \delta\hat{\tau}_n') & \text{(measurement)} \\[2ex] (I + JB_n) \, \delta\hat{\underline{x}}_n' & \text{(correction)} \end{cases} \qquad (2.46)
$$

The scalar coefficient a_n is computed from

$$
a_n = \underline{h}_n^T \, K^T \, E_n' \, K \, \underline{h}_n + \overline{a_n^2} \qquad (2.47)
$$

The rectangular matrix J is just the reverse of the K matrix so that

$$
J = \left\| \begin{matrix} 0 \\ I \end{matrix} \right\| \qquad (2.48)
$$

The matrix B_n is also rectangular and is defined as

$$
B_n = \left\| \begin{matrix} C_n^* & -I \end{matrix} \right\| \qquad (2.49)
$$

where C_n^* is one of the fundamental navigation matrices described in Ref. 1.

At each decision point the correlation matrix E_n must be updated. Thus

$$
E_n = \begin{cases} E_n' - a_n^{-1} (E_n' K\underline{h}_n)(E_n' K\underline{h}_n)^T & \text{(measurement)} \\[2ex] E_n' + J \, \overline{\underline{n}_n \underline{n}_n^T} \, J^T & \text{(correction)} \end{cases} \qquad (2.50)
$$

where $\underline{n}$ denotes the uncertainty in the velocity correction.

Eqs. (2.46) and (2.50) represent the recursive relation used in obtaining improved estimates of position and velocity deviation at each of the measurement times t_1, t_2..........

2.7 Solution of the Trajectory Equations

Let $r_s(t)$ and $v_s(t)$ denote the position and velocity vectors of the vehicle in an inertial coordinate system, and let $g(r_s,t)$ denote the gravitational acceleration at position r_s and time t. Now let $r_0(t)$ and $v_0(t)$ denote the position and velocity at time t associated with the prescribed reference trajectory. With this information we have

$$\delta r(t) = r_s(t) - r_0(t) \tag{2.51}$$

and

$$\delta v(t) = v_s(t) - v_0(t) \tag{2.52}$$

so that

$$\frac{d(\delta r)}{dt} = \delta v \tag{2.53}$$

and

$$\frac{d(\delta v)}{dt} = G(r_0,t)\,\delta r \tag{2.54}$$

where $G(r_0,t)$ is a matrix whose elements are the partial derivatives of the components of $g(r_0,t)$ with respect to

the components of $\underline{r}_0$. Define t_L and t_A as the time of launch and the time of arrival at the target.

To solve Eqs. (2.53) and (2.54) define the matrices

$$\frac{dR}{dt} = V, \quad \frac{dR^*}{dt} = V^*$$

$$\frac{dV}{dt} = GR, \quad \frac{dV^*}{dt} = GR^* \tag{2.55}$$

where

$$R(t_L) = 0 \ , \ R^*(t_A) = 0$$

$$V(t_L) = I \ , \ V^*(t_A) = I \tag{2.56}$$

so that

$$\delta\underline{r}(t) = R(t)\underline{c} + R^*(t)\underline{c}^* \tag{2.57}$$

and

$$\delta\underline{v}(t) = V(t)\underline{c} + V^*(t)\underline{c}^* \tag{2.58}$$

where $\underline{c}$ and $\underline{c}^*$ are arbitrary constant vectors.

2.8 Vector Velocity Corrections

Associated with the position $\underline{r}_s$ and the time t is the vector velocity required by the vehicle to travel in free fall from $\underline{r}_s(t)$ to the target point $\underline{r}_0(t_A)$ in the time interval $(t_A - t)$.

Solving Eqs. (2.57) and (2.58), it can be shown that

the required velocity deviations at time t can be written as

$$\delta \underline{v}^+(t) = V*(t)\ R*(t)^{-1}\ \delta \underline{r}(t) \qquad (2.59)$$

and

$$\delta \underline{v}^-(t) = V(t)\ R(t)^{-1}\ \delta \underline{r}(t) \qquad (2.60)$$

where the superscripts - and + denote the velocity just prior to or immediately following the correction respectively.

From Eq. (2.59) and (2.60) the required velocity correction $\Delta \underline{v}*$ is given as

$$\Delta \underline{v}*(t) = C*(t)\ \delta \underline{r}(t) - \delta \underline{v}^-(t)$$

$$= \left[C*(t) - C(t) \right]\ \delta \underline{r}(t) \qquad (2.61)$$

$$= -\Lambda(t)\ \delta \underline{v}(t_L)$$

where

$$C*(t) = V*(t)\ R*(t)^{-1} \qquad (2.62)$$

$$C(t) = V(t)\ R(t)^{-1} \qquad (2.63)$$

$$\Lambda(t) = V(t) - C*(t)\ R(t) \qquad (2.64)$$

$$\Lambda*(t) = V*(t) - C(t)\ R*(t) \qquad (2.65)$$

and $\delta \underline{v}(t_L)$ denotes an injection velocity error.

Finally it can be shown that

$$\delta \underline{x}(t) = \left\| \begin{matrix} R(t) & R*(t) \\ \\ V(t) & V*(t) \end{matrix} \right\| \ \left\| \begin{matrix} \underline{c} \\ \\ \underline{c}* \end{matrix} \right\| \tag{2.66}$$

and from Eq. (2.23) the six-dimensional transition matrix can be computed as

$$\Phi_{n+1,n} = \left\| \begin{matrix} R_{n+1} & R^*_{n+1} \\ \\ V_{n+1} & V^*_{n+1} \end{matrix} \right\| \ \left\| \begin{matrix} -\Lambda_n^{-1} & 0 \\ \\ 0 & -\Lambda_n^{*-1} \end{matrix} \right\| \ \left\| \begin{matrix} C^*_n & -I \\ \\ C_n & -I \end{matrix} \right\| \tag{2.67}$$

Using Eqs. (2.30) and (2.49), an estimate of the velocity correction vector $\delta \hat{\underline{v}}_n$ may be determined from

$$\Delta \hat{\underline{v}}_n = B_n \ \delta \hat{\underline{x}}_n \tag{2.68}$$

This process is necessary in that injection, measurement, and rocket instrumentation errors give rise to a series of velocity corrections to be implemented along the trajectory.

To distinguish times of velocity correction from decision point times, $t_{c,n}$ will be used to denote the time of the n-th correction maneuver. A commanded velocity change will be denoted as $\Delta \hat{\underline{v}}_{c,n}$, while $\Delta \underline{v}_{c,n}$ and $\underline{\eta}_{c,n}$ will denote the actual velocity change

experienced and the uncertainty in applying the correction respectively. Therefore, we can write

$$\Delta \hat{\underline{v}}_{c,n} = \Delta \underline{v}_{c,n} + \underline{\eta}_{c,n} \tag{2.69}$$

from which the actual velocity change may be expressed as

$$\Delta \underline{v}_{c,n} = B_{c,n} \, (\delta \underline{x}'_{c,n} \, \underline{e}_{c,n}) - \underline{\eta}_{c,n} \tag{2.70}$$

At the correction point

$$\underline{e}_{c,n} = \underline{e}'_{c,n} + \left\| \begin{matrix} 0 \\ \\ \underline{\eta}_{c,n} \end{matrix} \right\| \tag{2.71}$$

so that Eq. (2.70) becomes

$$\Delta \underline{v}_{c,n} = B_{c,n} (\delta \underline{x}'_{c,n} + \underline{e}_{c,n}) \tag{2.72}$$

Also the correlation matrix of the deviation errors must be updated at the correction point. It follows from Eq. (2.71) that

$$E_{c,n} = E'_{c,n} + \left\| \begin{matrix} 0 & 0 \\ 0 & \underline{\eta}_{c,n}\underline{\eta}^T_{c,n} \end{matrix} \right\| \tag{2.73}$$

Eq. (2.72) may be rewritten as

$$\Delta \underline{v}_{c,n} = B_{c,n} \, \underline{e}_{c,n} - \Lambda_{c,n} \, \Lambda^{-1}_{c,n-1} \, B_{c,n-1} \, \underline{e}_{c,n-1}$$

$$\tag{2.74}$$

or we may write

$$\Delta\hat{\underline{v}}_{c,n} = B_{c,n} \, \underline{e}'_{c,n} - \Lambda_{c,n} \, \Lambda^{-1}_{c,n-1} \, B_{c,n-1} \, \underline{e}_{c,n-1}$$

(2.75)

and it is one of these two latter forms that we shall use.

The correlation matrix of the estimated velocity correction vector is found by computing the mathematical expectation of the product of $\Delta\hat{\underline{v}}_{c,n}$ and its transpose. This matrix is written as $\Delta\hat{\underline{v}}_{c,n}\Delta\underline{v}^T_{c,n}$ from whose trace is defined the mean-squared estimate of the velocity correction.

The uncertainty associated with a velocity correction is defined as

$$\underline{d}_{c,n} = \Delta\hat{\underline{v}}_{c,n} - B_{c,n} \, \delta\underline{x}_{c,n}$$

(2.76)

$$= B_{c,n} \, \underline{e}'_{c,n}$$

from which the mean-squared uncertainty is determined as the trace of the matrix

$$\overline{\underline{d}_{c,n}\underline{d}^T_{c,n}} = B_{c,n} \, E'_{c,n} \, B^T_{c,n}$$

(2.77)

Since the inaccuracy in establishing a commanded velocity correction $\Delta\hat{\underline{v}}$ is due to errors in both magnitude and orientation, it is necessary to examine more carefully the vector uncertainty $\underline{\eta}$ in the velocity correction. Both

sources of error will be assumed independently random with zero means.

It can be shown that the uncertainty vector $\underline{\eta}$ is expressible as

$$\underline{\eta} = \Delta\hat{\underline{v}} - \Delta\underline{v} = -\Delta\hat{\underline{v}} \, M \left\{ (1 + k) \, \gamma \begin{Vmatrix} \cos\beta \\ \sin\beta \\ 0 \end{Vmatrix} + K \begin{Vmatrix} 0 \\ 0 \\ 1 \end{Vmatrix} \right\}$$

(2.78)

and the corresponding correlation matrix of the velocity correction uncertainty is

$$\overline{\underline{\eta}\underline{\eta}^T} = \overline{k^2} \, \overline{\Delta\hat{\underline{v}}\Delta\hat{\underline{v}}^T} + \overline{\frac{\gamma^2}{2}} \, \overline{\Delta\hat{v}^2} \, M \begin{Vmatrix} 1 & 0 & 0 \\ 0 & 1 & 0 \\ 0 & 0 & 0 \end{Vmatrix} M^T$$

(2.79)

$$= \overline{k^2} \, \overline{\Delta\hat{\underline{v}}\Delta\hat{\underline{v}}^T} + \overline{\frac{\gamma^2}{2}} \left(\overline{\Delta\hat{\underline{v}}^T \, \Delta\hat{\underline{v}}} \, I - \overline{\Delta\hat{\underline{v}} \, \Delta\hat{\underline{v}}^T} \right)$$

(2.80)

where I is the three-dimensional identity matrix, K is a random variable, M is a transformation matrix, γ is a random angle between $\Delta\hat{\underline{v}}$ and $\Delta\underline{v}$, β is a polar angle defining the rotation of $\Delta\underline{v}$ with respect to $\Delta\underline{v}$ and K, γ, and β are all statistically independent random variables with zero means.

2.9 Target Miss Distance

Denoting t_N as the time of the last velocity correction and $\delta \underline{x}_A$ as the deviation vector at the time of arrival t_A, it can be shown that

$$\delta \underline{r}_A = -R_A \Lambda_N^{-1} B_N \delta \underline{x}_N^+$$

$$= R_A \Lambda_N^{-1} B_N \underline{e}_N \tag{2.81}$$

which relates the target position error to the error vector $\underline{e}_N$. The mean-squared position error at the target is then the trace of the matrix $\overline{\delta \underline{r}_A \, \delta \underline{r}_A^T}$.

CHAPTER 3

OCCULTATION THEORY

3.1 Trajectory

The reference trajectory used in this study is the outbound half of a close approach, free fall, circum-lunar trajectory with departure on May 20, 1968.[3] The trajectory starts from an earth parking orbit at 114 miles. The distance to the moon's surface at the closest point of approach is 60 miles. The time from departure of the parking orbit to arrival at the closest point of approach is 62.5 hours.

3.2 Statistical Star Background

In order to base this study on actual occultations that would occur along the reference trajectory, a great quantity of star data would have to be compiled. Considering only stars of magnitude six or greater, it would be necessary to tabulate unit vectors for approximately 10,000 stars. Even with this information, the computation necessary to determine when occultations occur would be lengthy.

To avoid these difficulties a statistical star background

is employed. The stars are assumed to be distributed isotropically and at random. The star density is assumed to be a function of visual magnitude. The star densities used in this study are tabulated as a function of visual magnitude for magnitudes four through nine in Table 3.1. In each case the density is given for stars brighter than the corresponding magnitude.

TABLE 3.1

STATISTICAL STAR DENSITY AS A FUNCTION OF
VISUAL MAGNITUDE [4]

Magnitude (Mag)	Star Density* (CF_I)	$\log_{10} d$
4	0.0129	-1.89
5	0.0398	-1.40
6	0.1175	-0.93
7	0.3467	-0.46
8	1.000	0.00
9	2.818	0.45

*density of stars brighter than the corresponding magnitude

3.3 Occultation Frequency Assumptions

For an actual flight occultation times would normally be precalculated so that the approximate time of each useful occultation would be known in advance. Measurements would

then be made as the useful occultations occur. To simulate this procedure accurately on the basis of a statistical star background it would be necessary to determine a specific time of occurrence for every occultation. Since trajectory data is given at intervals along the trajectory known as "decision points", it is advantageous to make all calculations at these decision points. For this reason the frequency of occultation will be determined at each decision point, and the assumption will be made that the frequency of occultation remains constant until the next decision point is reached at which time a new occultation frequency will be computed. This approximation is entirely satisfactory for the purpose of this study since the interval between decision points ranges from 1.2 to 30 minutes corresponding to portions of the trajectory that are near either body or far from both bodies respectively.

In determining the frequency of occultations the earth and the moon are assumed to be perfect spheres, and the periphery of either body is assumed to be illuminated or not illuminated with no gradation. The state of illumination is based on light from the sun only. Reflected light is not considered.

3.4 Determination of Occultation Frequency

The following derivation is taken largely from an unpublished study by Dr. J. H. Laning Jr.[2]
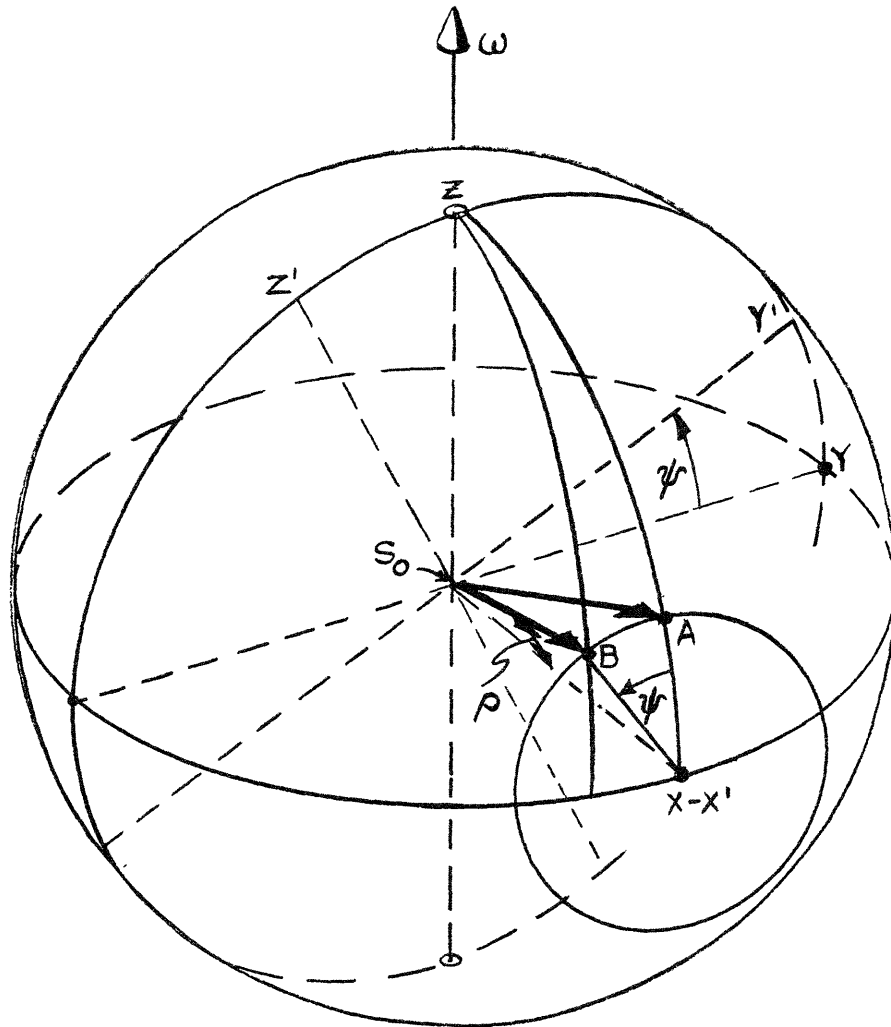
Fig. 3.1 Star occultation geometry

In the work that follows an underscore will be used to indicate a vector quantity. When the underscore is omitted from a previously defined vector quantity, it will be understood that the magnitude is meant.

Let $\underline{A}$ be a unit vector with x, y, z components $\cos\rho$, 0, $\sin\rho$. Let $\underline{B}$ be a unit vector having x', y', z' components

$\cos \rho$, 0, $\sin \rho$. From Fig. 3.1 it can be seen that

$$x = x'$$
$$y = y' \cos \psi - z' \sin \psi = - \sin \rho \sin \psi \qquad (3.1)$$
$$z = y' \sin \psi + z' \cos \psi = - \sin \rho \cos \psi$$

so that $\underline{B}$ has components in the x, y, z frame of $\cos \rho$, $-\sin \rho \sin \psi$, $\sin \rho \cos \psi$.

As seen from the spacecraft, stars are occulted by a body due to two effects: the apparent angular velocity of the line of sight from the spacecraft to the body and the apparent expansion and contraction of the body due to a velocity component toward or away from it. Since the angular velocity of the line of sight is given by

$$\underline{\omega} = \omega \underline{z} \qquad (3.2)$$

the motion of B due to the angular velocity of the line of sight is

$$\underline{\omega} \times \underline{B} = \omega (\underline{z} \times \underline{x} \cos \rho - \underline{z} \times \underline{y} \sin \rho \sin \psi)$$
$$= \omega \underline{y} \cos \rho + \omega \underline{x} \sin \rho \sin \psi \qquad (3.3)$$

The motion of B due to radial motion of the spacecraft with

respect to the body is

$$- \dot{\rho} \ (\underline{y}' \ x \ \underline{B}) = - \dot{\rho} \ (\underline{y} \cos \psi + \underline{z} \sin \psi) x \ \underline{B}$$

$$= - \dot{\rho} \begin{vmatrix} \underline{x} & \underline{y} & \underline{z} \\ 0 & \cos \psi & \sin \psi \\ \cos \rho & -\sin \rho \ \sin \psi & \sin \rho \ \cos \psi \end{vmatrix}$$

$$= - \dot{\rho} \left[\underline{x} \ (\cos^2 \psi \ \sin \rho + \sin^2 \psi \ \sin \rho) \right.$$

$$+ \ \underline{y} \ (\sin \psi \ \cos \rho) + \underline{z} \ (-\cos \psi \ \cos \rho) \left. \right]$$

$$= - \dot{\rho} \ \underline{x} \ \sin \rho - \dot{\rho} \ \underline{y} \ \sin \psi \ \cos \rho + \dot{\rho} \ \underline{z} \ \cos \psi \ \sin \rho$$

$$(3.4)$$

Adding the motion of B due to each of the effects mentioned will yield the total motion of B.

$$\underline{v}_B = \underline{x} \ (- \dot{\rho} \ \sin \rho + \omega \ \sin \psi \ \sin \rho) + \underline{y} \ (- \dot{\rho} \ \sin \psi \ \cos \rho$$

$$+ \ \omega \ \cos \rho + \underline{z} \ (\dot{\rho} \ \cos \psi \ \cos \rho) \qquad (3.5)$$

The total motion of B can now be broken into two components: (1) the component along the line of sight to B which does not contribute to the sweeping out of star background; and (2) the radial component (radial with respect to the occulting body) which does sweep out an area of the star background. To facilitate the separation of

the radial component it is convenient to define a unit vector in the direction of radial motion.

$$u = - \underline{x} \sin \rho + \underline{x}' \sin \rho$$

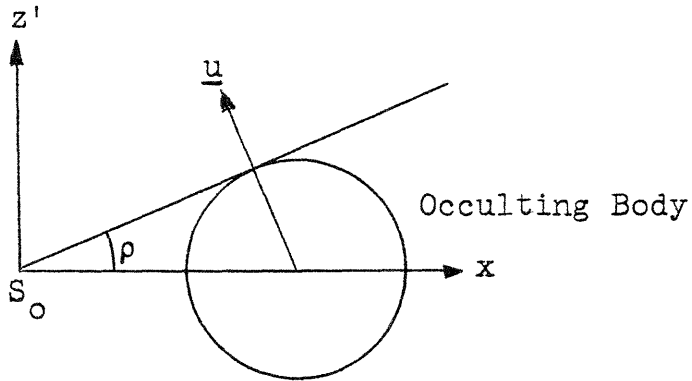$$= - \underline{x} \sin \rho + \cos \rho \ (- \underline{y} \sin \psi \ \underline{z} \cos \psi) \tag{3.6}$$

Fig. 3.2   Unit vector in direction of radial motion

The radial component of motion of B is given by

$$v_{B_R} = \underline{v}_B \cdot \underline{u} = (- \dot{\rho} \sin \rho + \omega \sin \psi \sin \rho)(- \sin \rho)$$

$$+ (- \dot{\rho} \sin \psi \cos \rho + \omega \cos \rho)(- \sin \psi \cos \rho)$$

$$+ (\dot{\rho} \cos \psi \cos \rho)(\cos \psi \cos \rho)$$

$$= \dot{\rho} \left[\sin^2 \rho \cos^2 \rho \ (\sin^2 \psi + \cos^2 \psi) \right]$$

$$+ \omega \ (- \sin \psi \sin^2 \rho - \sin \psi \cos^2 \rho)$$

$$= \dot{\rho} - \omega \sin \psi \tag{3.7}$$

Thus the rate at which an element $d\psi$ along the visible

periphery of the body sweeps out the star background is

$$\dot{A} = (\dot{\rho} - \omega \sin \psi) \sin \rho \; d\psi \qquad (3.8)$$

It is necessary to express $\dot{A}$ in terms of parameters that will be available at each decision point. The following quantities are available:

$\underline{R}$ - the vector from the center of the reference body to the spacecraft

$\underline{V}$ - the velocity of the spacecraft with respect to the reference body

R_{EM} - the vector from the center of the earth to the center of the moon

V_{EM} - the velocity of the moon with respect to the earth

Knowledge of these quantities, along with the radius of the occulting body, is sufficient for the computation of all the quantities shown in Fig. 3.3.
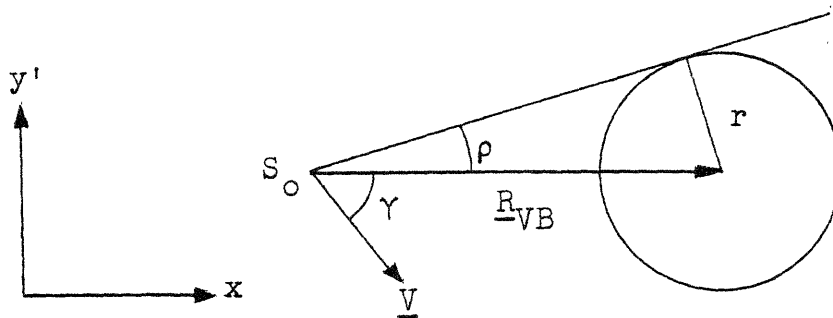
Fig. 3.3 Star occultation geometry

With the aid of Fig. 3.3 the following relations are readily developed:

$$\sin \rho = \frac{r}{R_{VB}} \tag{3.9}$$

$$\dot{\rho} \cos \rho = -r \frac{\dot{R}_{VB}}{R_{VB}^2}$$

$$\dot{\rho} = -\tan \rho \frac{\dot{R}_{VB}}{R_{VB}} \tag{3.10}$$

$$\dot{R}_{VB} = - V \cos \gamma \tag{3.11}$$

$$\dot{\rho} = \frac{V}{R_{VB}} \tan \gamma \cos \gamma \tag{3.12}$$

$$\omega = \frac{V}{R_{VB}} \sin \gamma \tag{3.13}$$

Therefore

$$\dot{A} = \frac{V \sin \rho}{R_{VB}} \left[\tan \rho \cos \gamma - \sin \psi \sin \gamma \right] d\psi \tag{3.14}$$

The portion of a body that occults a star may be illuminated or dark. In addition the body may be covering or uncovering the star. The accuracy with which the time of occultation can be observed is dependent upon both these conditions. For this reason it would be convenient to sort occultations into four categories, covering all combinations of the above conditions. This can be accomplished during the integration around the periphery of the occulting body with respect to $d\psi$. The integration will be separated

into four parts corresponding to the four conditions:

NI+ non-illuminated, covering previously visible sky

NI- non-illuminated, uncovering previously hidden sky

I+ illuminated, covering previously visible sky

I- illuminated, covering previously hidden sky

The covering or uncovering category is determined by the sign of $\dot{A}$. In order to determine the illumination condition the direction from the occulting body to the sun must be established. The vector from the sun to the earth $\underline{R}_{SE}$ is part of the information available at each decision point. Depending on which body is the occulting body, the unit vector from the occulting body to the sun $\underline{U}_S$ can be established.

Now define a unit vector $\underline{U}_{OB}$ along the direction from the center of the occulting body to a point on the visible periphery determined by the value of ψ as shown in Fig. 3.4 where

$$\underline{U}_{OB} = - \sin \rho \ \underline{x} - \cos \rho \sin \psi \ \underline{y} + \cos \rho \cos \psi \ \underline{z} \qquad (3.15)$$

Thus

$$\underline{U}_{OB} \cdot \underline{U}_S > 0 \qquad (3.16)$$

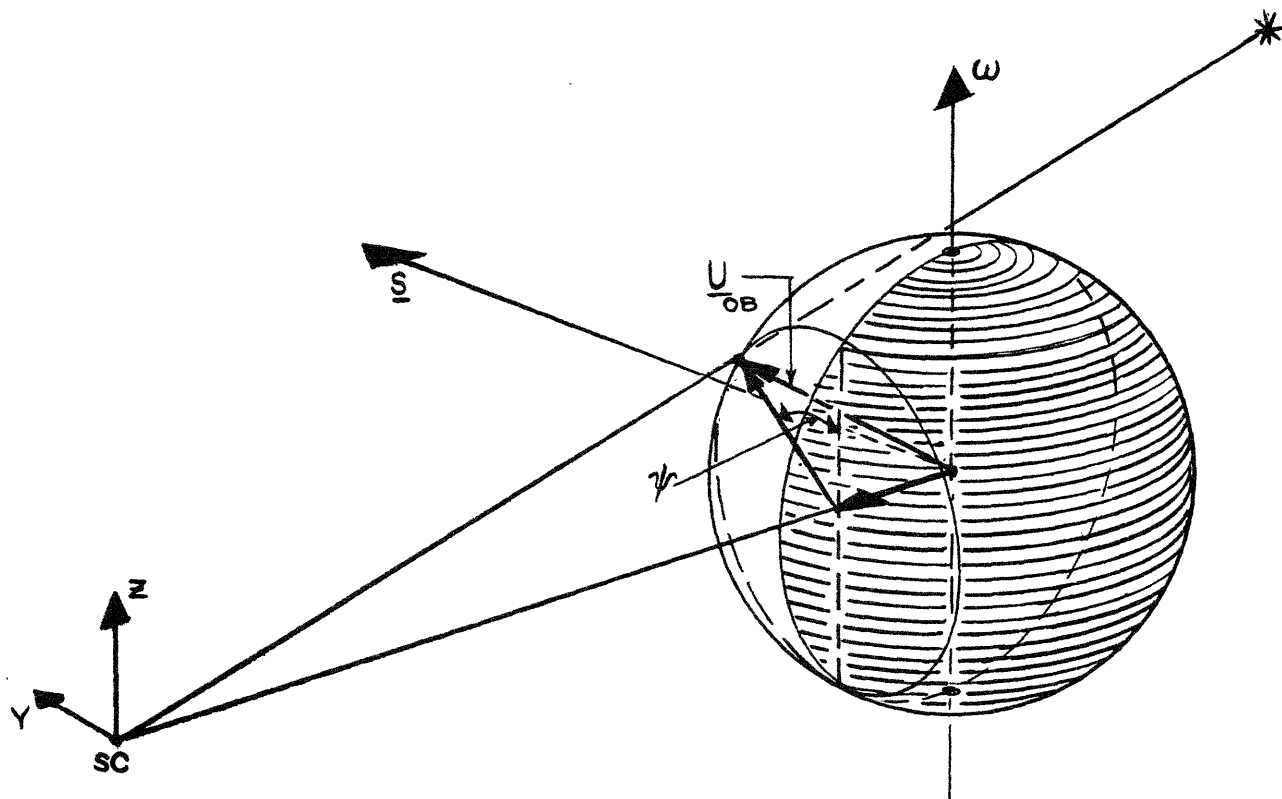indicates that the periphery in the direction $\underline{U}_{OB}$ from the

Fig. 3.4 Occulting body illumination

center of the occulting body is illuminated and

$$\underline{U}_{OB} \cdot \underline{U}_S < 0 \tag{3.17}$$

indicates a non-illuminated condition. Integrating $\dot{A}$ over

the visible periphery, keeping track of four categories of

occultations, results in four corresponding values for the

rate at which the statistical star background is being

swept out. If Q_0, Q_1, Q_2 and Q_3 correspond to NI +, NI -,

I +, and I - respectively, the frequency of occultation in each category may be found by

$$FREQ_0 = CF_I \; Q_0 \qquad (3.18)$$

$$FREQ_1 = CF_I \; Q_1 \qquad (3.19)$$

$$FREQ_2 = CF_I \; Q_2 \qquad (3.20)$$

$$FREQ_3 = CF_I \; Q_3 \qquad (3.21)$$

where CF_I is a conversion factor dependent on the magnitude of stars being considered and the units of Q. See Table 3.1. It should be noted that the preceding calculations are gone through twice at each decision point, once for the earth as the occulting body and once for the moon as the occulting body.

3.5 Random Number Method for Determining Whether an Occultation Occurs

$FREQ_0$ through $FREQ_3$ represent the average frequency with which occultations of the corresponding category are taking place during the time interval between two decision points. Based on this average frequency and the time interval involved, the number of occultations in each of the four categories can be determined. However, for the purpose of this study a simpler computation is adequate. It is assumed that only one observation will be made between decision points, regardless of the number of occultations that occur.

The navigational value of an occultation depends chiefly on the orientation of the bodies involved and the category of the occultation. Since the orientation of the bodies remains essentially constant during the time interval between two decision points, all observations subsequent to the first one would provide essentially redundant information.

The probability that a specific number of occultations occurs between two decision points is given by a Poisson distribution. For example, the probability that two occultations of type NI $+$ occur in the interval $t_2 - t_1$ is given by

$$P_2 = \frac{\mu^2}{2!} e^{-\mu} \tag{3.22}$$

where

$$\mu = (FREQ_0)(t_2 - t_1) \tag{3.23}$$

Since only one measurement will be made regardless of the number of occultations that occur it is necessary only to compute the probability, P_{nz}, that one or more occultations occur. This is accomplished by finding the probability that no occultations occur and subtracting this result from one.

$$P_{nz} = 1 - \frac{\mu^0}{0!} e^{-\mu} = 1 - e^{-\mu} \tag{3.24}$$

The occurrence or non-occurrence of an occultation is then determined in the following manner.

A random number with rectangular distribution and an interval of zero to one is generated. P_{nz} is subtracted from this random number. A negative or zero result is interpreted as meaning that one or more occultations occur in the time interval under consideration.

This computation is made eight times at each decision point. It is performed for each of eight values of FREQ, corresponding to two occulting bodies with four categories of occultations each. The result is

$$OCC_{E,0} = 0 \text{ or } 1$$
$$OCC_{E,1} = 0 \text{ or } 1$$
$$\vdots$$
$$OCC_{M,3} = 0 \text{ or } 1$$

(3.25)

where subscripts E and M represent the earth and moon respectively, and the zero or one represent the non-occurrence or occurrence of one or more occultations. In the event that no occultations occur at a decision point, the next decision point is examined. If one or more categories of occultation occur it is necessary to select the best one.

3.6 Selection of the Best Occultation

From the eight possible occultations the best two can be selected a priori. That is, the best occultation for

each body can be determined with no further calculation.
By '"best occultation'" is meant the occulation which yields
the most navigational information. It is obvious that a
NI + occultation is better than a I - occultation. The
choice between NI - and I + is not so obvious, but the
illumination condition is assumed to be the more important
for the purpose of this study. Thus the best occultation
for each body is the first type that occurs in the following
order of preference: NI +, NI -, I +, I -.

If both the earth and the moon provide occultations at
a particular decision point the choice between them is based
on the quantity ζ, defined as the mean squared reduction in
position error at the target if a velocity correction were
made following the measurement. The "best occultation" is
the one giving the largest ζ. This "best occultation" is the
occultation upon which further navigational computations
are based.

3.7 Determination of the Unit Vector from the Spacecraft to the Point of Occultation

Having identified the '"best occultation'" at a particular
decision point it is now necessary to determine the direction
from the spacecraft to the point of occultation. Since the
star field is being simulated by a statistical star
background it will be necessary to locate the point of
occultation by a random number process.

The angular velocity of the line of sight to the occulting body is given by

$$\underline{\omega}_{OB} = \frac{(\underline{R}_{VB} \times \underline{V}_{OB})}{R_{VB}^2} \qquad (3.26)$$

where $\underline{R}_{VB}$ is the vector from the spacecraft to the center of the occulting body, and $\underline{V}_{OB}$ is the velocity of the occulting body with respect to the spacecraft. The direction orthogonal to $\underline{\omega}_{OB}$ and $\underline{R}_{VB}$ is defined as $\underline{A}$ where

$$\underline{A} = \underline{\omega}_{OB} \times \underline{R}_{VB} \qquad (3.27)$$

$\underline{A}$ and $\underline{R}_{VB}$ lie in the plane of Fig. 3.5
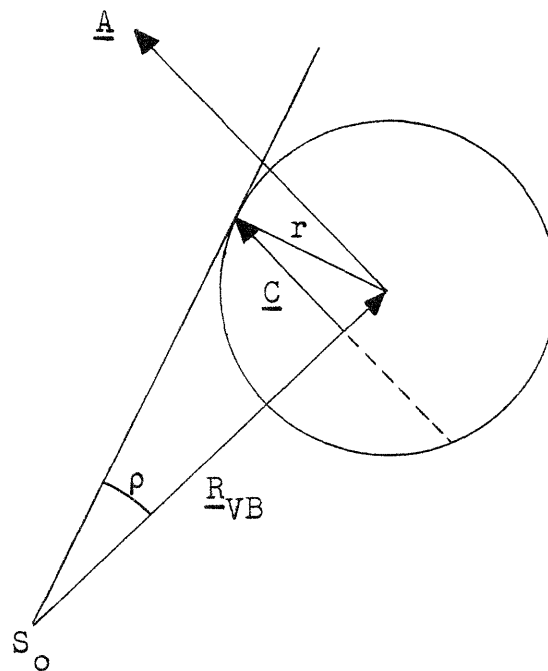

Fig. 3.5 Apparent semi-diameter of the occulting body

The apparent semi-diameter of the occulting body, C, is given by

$$C = r \cos \rho \qquad (3.28)$$

and the vector $\underline{C}$, shown in Fig. 3.5 is given by

$$\underline{C} = \frac{C\underline{A}}{A} \qquad (3.29)$$

A cross section of the occulting body containing $\underline{C}$ and $\underline{\omega}$ is shown in Fig. 3.6.
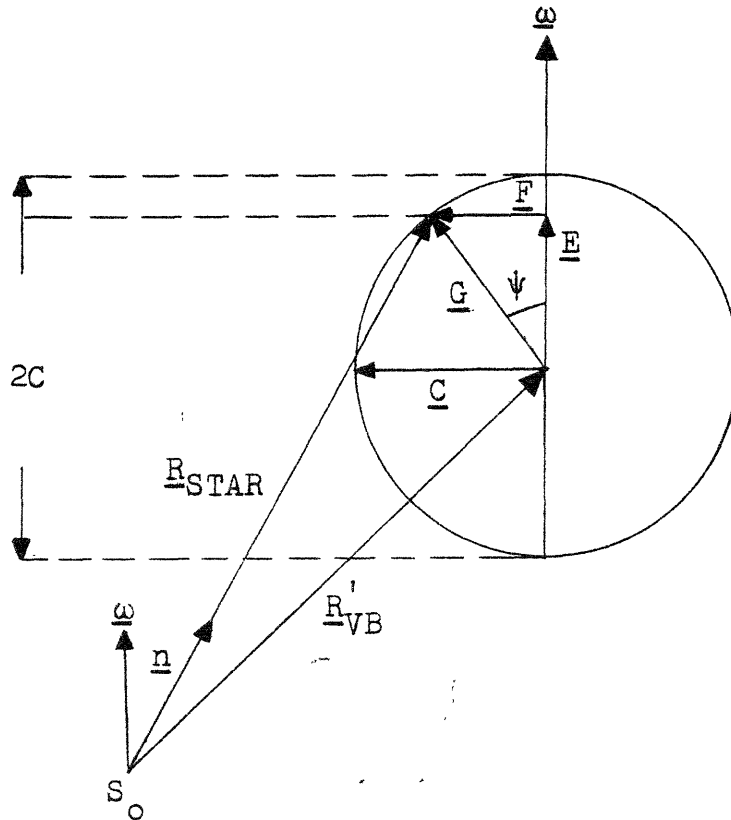

Fig. 3.6 Geometry for determining the point of occultation

From Fig. 3.5 it can be seen that

$$\underline{R}'_{VB} = \cos^2 \rho \, \underline{R}_{VB} \tag{3.30}$$

where $\underline{R}'_{VB}$ is the vector from the spacecraft to the center of the visible disk.

A rectangularly distributed random number T is now generated with width - C to + C. Thus T determines the magnitude and direction of $\underline{E}$ in accordance with the original hypothesis that the stars are isotropically and randomly distributed.

$$\underline{E} = T \, \frac{\underline{\omega}}{\omega} \tag{3.31}$$

$\underline{F}$ is found from the relation

$$\underline{F} = \sin \psi \, \underline{C} \tag{3.32}$$

and $\underline{G}$ is given by

$$\underline{G} = \underline{E} + \underline{F} \tag{3.33}$$

This leads to

$$\underline{R}_{STAR} = \underline{R}'_{VB} + \underline{G} \tag{3.34}$$

and finally

$$\underline{n} = \frac{\underline{R}_{STAR}}{R_{STAR}} \tag{3.35}$$

3.8 Visibility of Occultations

There are two limitations on the visibility of an occultation which must be taken into consideration. An occultation will not be observable if the line of sight to the occultation is too close to the line of sight to the sun. A limit of 15 degrees was used in this study. The computation

$$\text{TEST} = \underline{n} \cdot \underline{U}_{SUN} - \cos 15^{\circ} \tag{3.36}$$

where $\underline{n}$ and $\underline{U}_{SUN}$ are unit vectors to the occulted star and the sun, is used to determine if the lines of sight are within 15 degrees of each other. If TEST is positive the occultation is considered not visible.

The second condition affecting the visibility of an occultation is the position of the non-occulting body relative to the line of sight from the spacecraft to the point of occultation on the occulting body as shown in Fig. 3.7. $\underline{R}_n$ is the vector from the spacecraft to the center of the non-occulting body. The apparent radius of the non-occulting body θ is determined in the following manner

$$\theta = \arcsin \left[\frac{r_n}{R_n} \right] \tag{3.37}$$

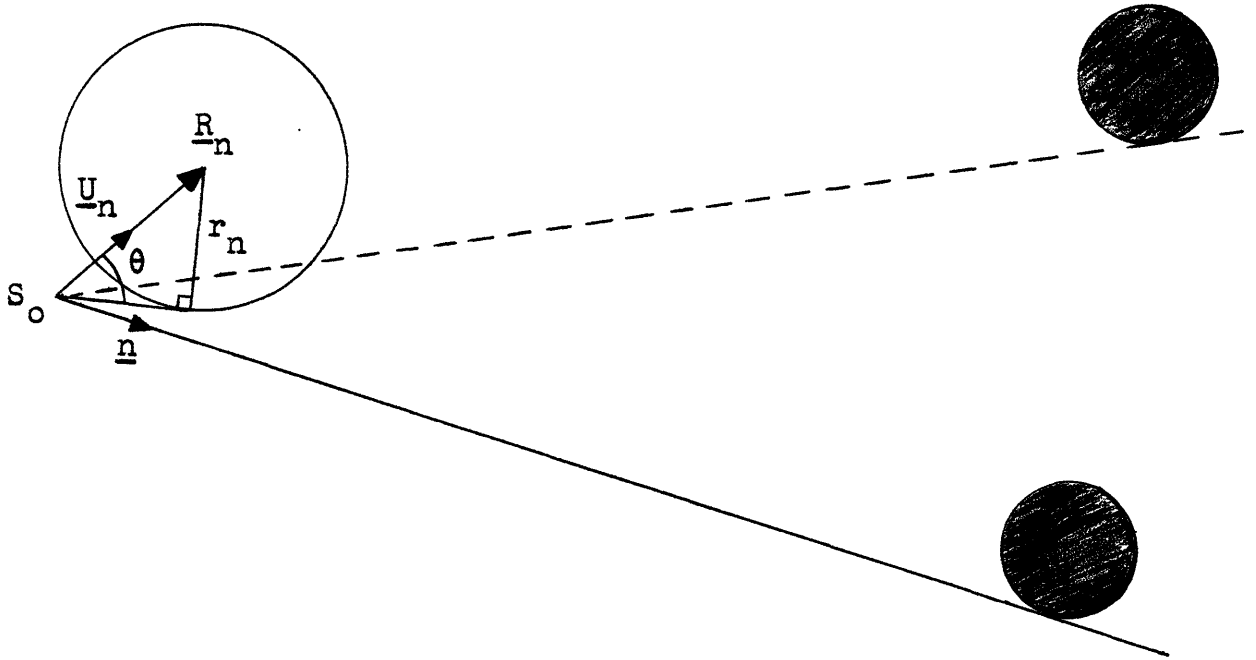Let $\underline{U}_n$ be the unit vector in the $\underline{R}_n$ direction. From

Fig. 3.7 Visibility of occultation

Section 3.7 the direction to the star being oculted is given by the vector $\underline{n}$.   Then

$$TEST = \underline{n} \cdot \underline{U}_n - \cos \theta \qquad (3.38)$$

From Fig. 3.7 it can be seen that TEST will be positive when the occultation is not visible.

3.9 Variance

The variance is a measure of the accuracy with which an occultation can be observed.   There are three factors which influence the variance.   The first, t_r, is the response time of the person making the observation.   This parameter is one

of the variable inputs to the program so that the effect of
of varying t_r can be studied. A nominal value for this
parameter is 0.2 seconds.

The second factor, t_c, compensates for the greater
difficulty in accurately observing occultations of the
NI-, I+ and I- types.

The third factor takes into consideration the deviation
of the occulting bodies from perfect spheres. The variation
from the assumed radius is given by

$$\delta r = R_{VB} \cos \rho \ \delta \rho \qquad (3.39)$$

or

$$\delta \rho = \frac{\delta r}{R_{VB} \cos \rho} \qquad (3.40)$$

Relating $\delta \rho$ to the variation in time,

$$\delta \tau = \frac{R_{VB} \cos \rho \ \delta \rho}{R_{VB} \cos \rho \ \omega \sin \psi} = \frac{R_{VB} \ \delta \rho}{v_r \sin \psi} \qquad (3.41)$$

Substituting Eq. (3.40) into Eq. (3.41)

$$\delta \tau = \frac{\delta r}{v_r \cos \rho \sin \psi}$$

It should be noted that δr will depend on the occulting
body. δr_e and δr_m are used to represent the variation of the

earth's surface and the moon's surface respectively from their assumed radii.

The total variance is the sum of the squares of the three contributions. For the earth

$$V = t_r^2 + (K\ t_c)^2 + \left[\frac{\delta r_e}{v_r \cos \rho \sin \psi} \right]^2 \qquad (3.43)$$

and for the moon

$$V = t_r^2 + (K\ t_c)^2 + \left[\frac{\delta r_m}{v_r \cos \rho \sin \psi} \right]^2 \qquad (3.44)$$

where K has values 0, 1, 2 or 3 corresponding to the types of occultations NI +, NI -, I + and I -.

3.10 Determination of "h" Vector

From Chapter 2 the "h" vector for a star occultation is given by

$$h = - \frac{1}{(\underline{p} - \tan \gamma\ \underline{m}) \cdot \underline{v}_r} (\underline{p} - \tan \gamma\ \underline{m}) \qquad (3.45)$$

where $\underline{m}$ is the unit vector directed from the spacecraft to the center of the occulting body; γ is the angle between $\underline{m}$ and $\underline{n}$, the unit vector directed toward the point of occultation; $\underline{p}$ is the unit vector perpendicular to $\underline{m}$ and in the plane determined by $\underline{m}$ and $\underline{n}$ and $\underline{v}_r$ is the velocity of the spacecraft relative to the occulting body.

In terms of quantities derived up to this point the "h"
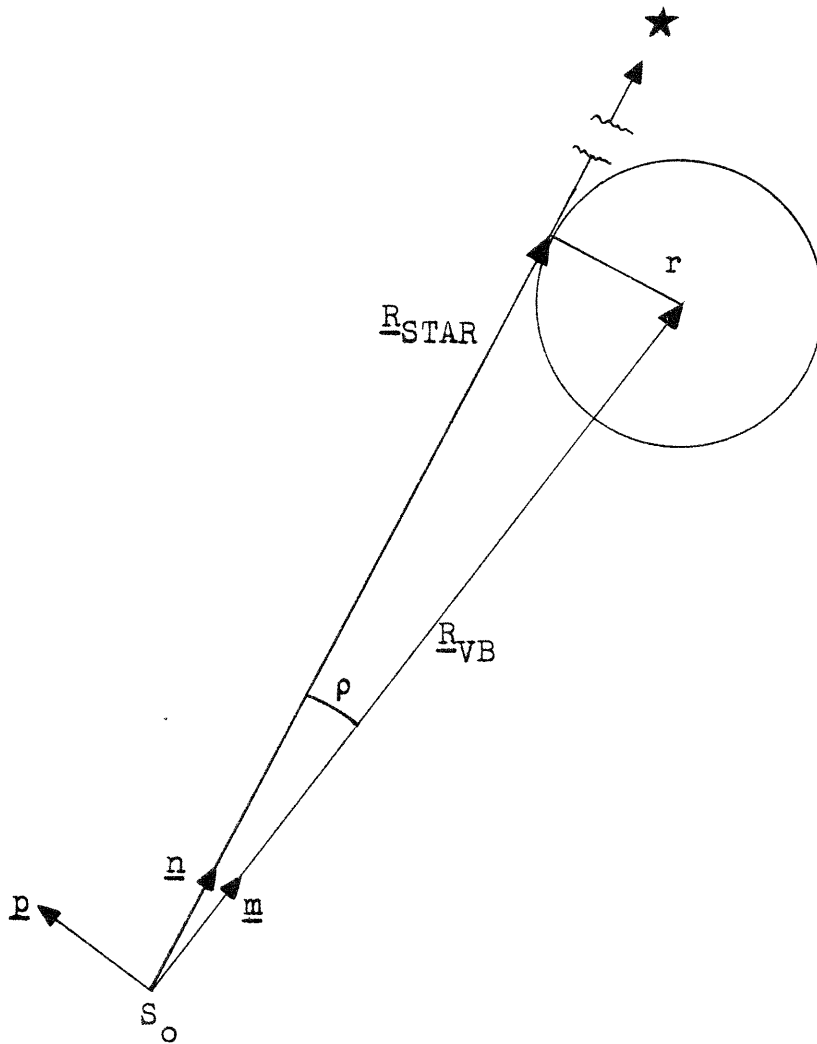fector is found as follows.

Fig. 3.8 "h" vector geometry

$$\underline{m} = \frac{\underline{R}_{VB}}{R_{VB}} \qquad\qquad (3.46)$$

The unit vector $\underline{l}$ is given by

$$\underline{l} = \frac{\underline{m} \times \underline{n}}{\sin \rho} \qquad (3.47)$$

and the unit vector $\underline{p}$, equivalent to $\underline{\rho}$ in Eq. 3.45 is then

$$\underline{p} = \underline{l} \times \underline{m} \qquad (3.48)$$

Rewriting Eq.(3.45) in terms of the quantities shown in Fig. 3.8 we have

$$h = - \frac{1}{(\underline{p} - \tan \rho \; \underline{m}) \cdot v_r} (\underline{p} - \tan \rho \; \underline{m}) \qquad (3.49)$$

CHAPTER 4

PRESENTATION AND DISCUSSION OF RESULTS

4.1 Introduction

The results obtained from the computations described in
Chapters 2 and 3 are strongly dependent on a number of
parameters, some of which could not be specified exactly by
the authors. For example, the value of δr_e (the contribution
to the variance in earth occultation measurements due to the
effect of the atmosphere and the departure of the earth's
surface from a regular geometry) was assumed to be eight
miles in all computations but one. In order to establish
this parameter more accurately a study of the optics
involved would have to be undertaken. In addition it would
be appropriate to determine to what extent this contribution
to the variance can be predicted, since any predictable
contribution could be compensated for in the calculations
and would not detract from the accuracy of an observation.
The results also depend on input conditions such as the
magnitude of stars used and the position of the sun. And
finally, the results vary with the mode of navigation
employed.

In the interest of both time and economy it was
necessary to make a limited number of computer runs. The
input conditions were varied over reasonable limits, and
the results are presented here in both tabular and
graphical form. Sufficient data is presented so that the
relative sensitivity or insensitivity of the results to
various input conditions can be determined. Thus, with
care, the data can be extrapolated to some degree to
cover cases for which computations were not made.

The results obtained by navigation schemes such as
the ones employed here, are highly dependent upon the
number and magnitudes of the velocity corrections and
the times at which they are implemented. No attempt was
made to optimize the application of velocity corrections.
Rather, the same decision rules were used for all runs
so that the results can be compared independent of the
method of determining when to make velocity corrections.
In all runs a velocity correction was made whenever the
ratio of the uncertainty in the computed velocity
correction to the computed velocity correction became
less than 0.2.

The results are also dependent on the injection
errors. These errors are specified by the value of the
initial "E matrix." The following value was assumed

for all runs.

$$E_0 = \begin{Vmatrix} .980 & .063 & .203 & 0 & 0 & 0 \\ .063 & 4.58 & -1.86 & 0 & 0 & 0 \\ .203 & -1.86 & 7.04 & 0 & 0 & 0 \\ 0 & 0 & 0 & 7.73 & 4.65 & 2.72 \\ 0 & 0 & 0 & 4.65 & 83.8 & 36.0 \\ 0 & 0 & 0 & 2.72 & 36.0 & 36.1 \end{Vmatrix}$$

This corresponds to a RMS positron error of 3.55 miles and a RMS velocity error of 11.3 miles.

4.2 Dependence of Results on the Random Number Sequence

As was explained in Chapter 3, there can be as many as four computations at each decision point which use the computer's random number function. Thus, the results of each run depend to some extent on the starting point in the random number sequence. It would be desirable to show that this dependence is such that the results are essentially independent of the starting point in the random number sequence. Table 4.1 shows the results of three runs in which all parameters were held constant with the exception of the starting point in the random number sequence.

TABLE 4.1

EFFECT OF VARYING THE STARTING POINT IN THE RANDOM
NUMBER SEQUENCE

Sun rotation 70
Magnitude < 4
Occultations and angle measurements

Run	Total Velocity Correction (mph)	Final Velocity Uncertainty (mph)	Final Position Uncertainty (miles)	Final Miss Distance (miles)
1	48.6	3.80	1.77	4.09
2	47.8	2.57	1.25	3.83
3	50.7	2.27	1.13	3.03

4.3 Navigation Modes

A number of navigation modes were considered in this
study. Navigation by angle measurements only, mode 1,
will be used as a basis for comparison, since this mode
of navigation has been studied extensively at the M.I.T.
Instrumentation Laboratory by the Space Guidance Analysis
Group. In order to obtain a more accurate comparison,
the best and worst cases of navigation by angle
measurements only are presented. These best and worst
cases result from values for sun rotation of 250 and 70
degrees respectively. The input parameter "sun

rotation" is used to vary the direction of the sun as viewed from earth. This device serves to simulate the illumination conditions that would be encountered at various times during the year without generating a new trajectory for each new time. The inaccuracies introduced by this device are not significant in this type of analysis. Navigation by occultations only, mode 2, will also be considered. The remaining mode, mode 3, involves using both occultation and angle measurements. All three basic modes are considered for a sun rotation of 70 and 250 degrees.

Two variations to the basic modes were introduced: (1) In two mode 3 runs the variance associated with occultation measurements was reduced in order to determine the sensitivity of the results to the accuracy with which occultation measurements can be made. In this case the astronaut's response time was reduced from 0.2 to 0.1 seconds. t_c, a factor which compensates for the difficulty in accurately observing occultations of types NI-, I+ and I-, was reduced from 0.2 to 0.1 seconds. δr_e was reduced from eight miles to one mile, and δr_m was reduced from three to 0.5 miles.[5] (2) In an effort to simulate a realizable navigation technique more closely, modes 2 and 3 were varied in one case to consider occultations of all types by the moon only and in a second case to consider only occultations of type NI+ by the moon.

4.4 Occultation Frequency

The frequency with which stars of magnitude less
than six are occulted by the earth and the moon is shown
in Fig. 4.1. The corresponding data for stars of magnitude
less than four are shown in Fig. 4.2. In both cases the
frequencies were computed for the first half of a
circumlunar voyage using the trajectory described in
Chapter 3 and shown in Fig. 4.3. The frequencies shown
in Figs. 4.1 and 4.2 are the total frequencies of
occultation. These total frequencies were obtained by
summing the results of Eqs. (3.18) through (3.21).
In Fig. 4.1 the influence of the spacecraft's position and
motion relative to the occulting bodies is shown quite
clearly. The initial occultation frequency for stars
of magnitude less than six occulted by the earth is
3102 occultations per hour. This extreme value, too
large to be shown in Fig. 4.1, is due to two factors:
(1) the nearness of the spacecraft to the earth; and
(2) the high rate at which the earth's periphery is
moving relative to the star background. The same effect
is noted when the spacecraft is at its closest point of
approach to the moon, the extreme lunar occultation
frequency being 4361 occultations per hour.

As the spacecraft starts around the far side of
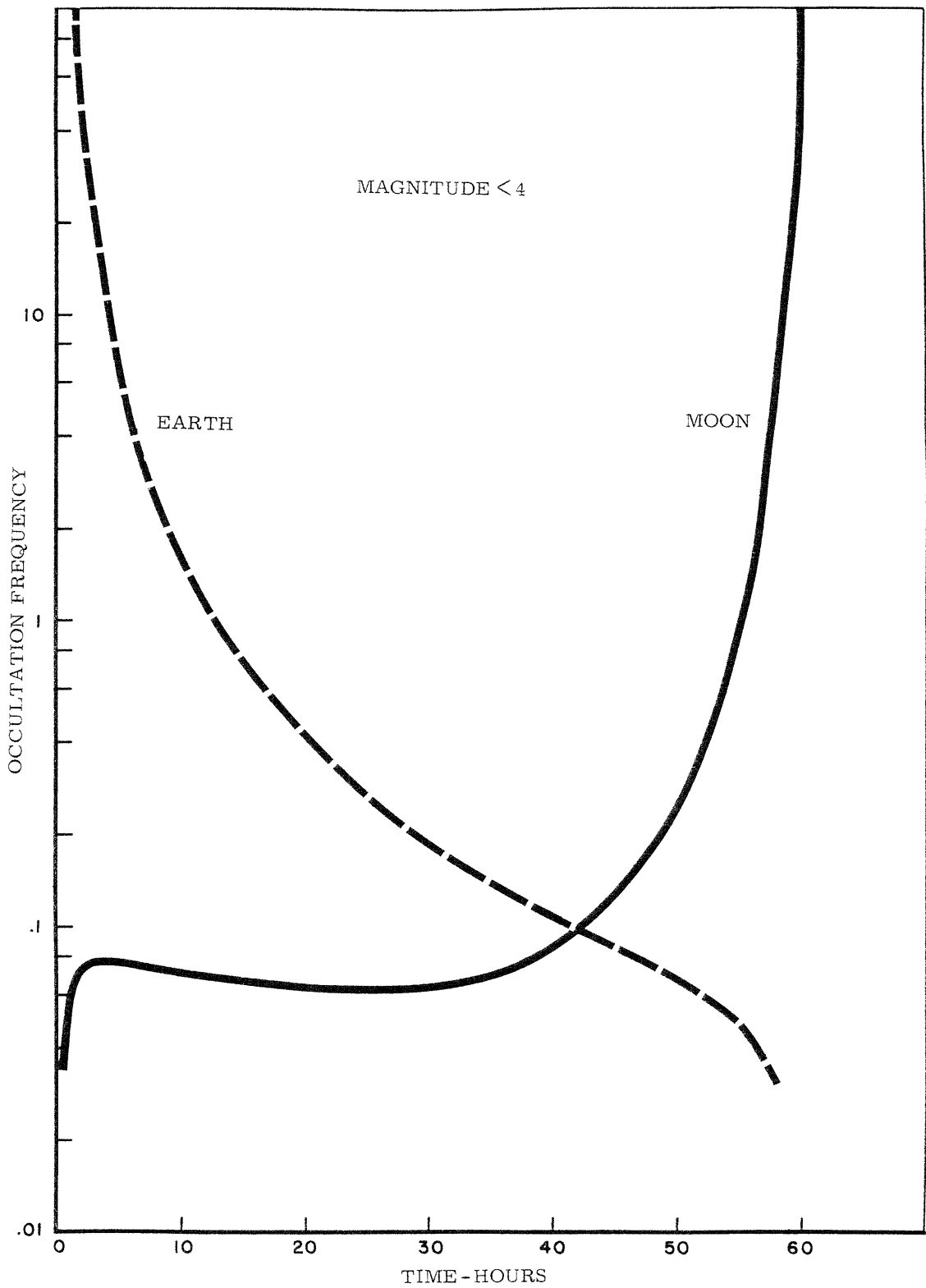the moon the frequency of occultations by the earth
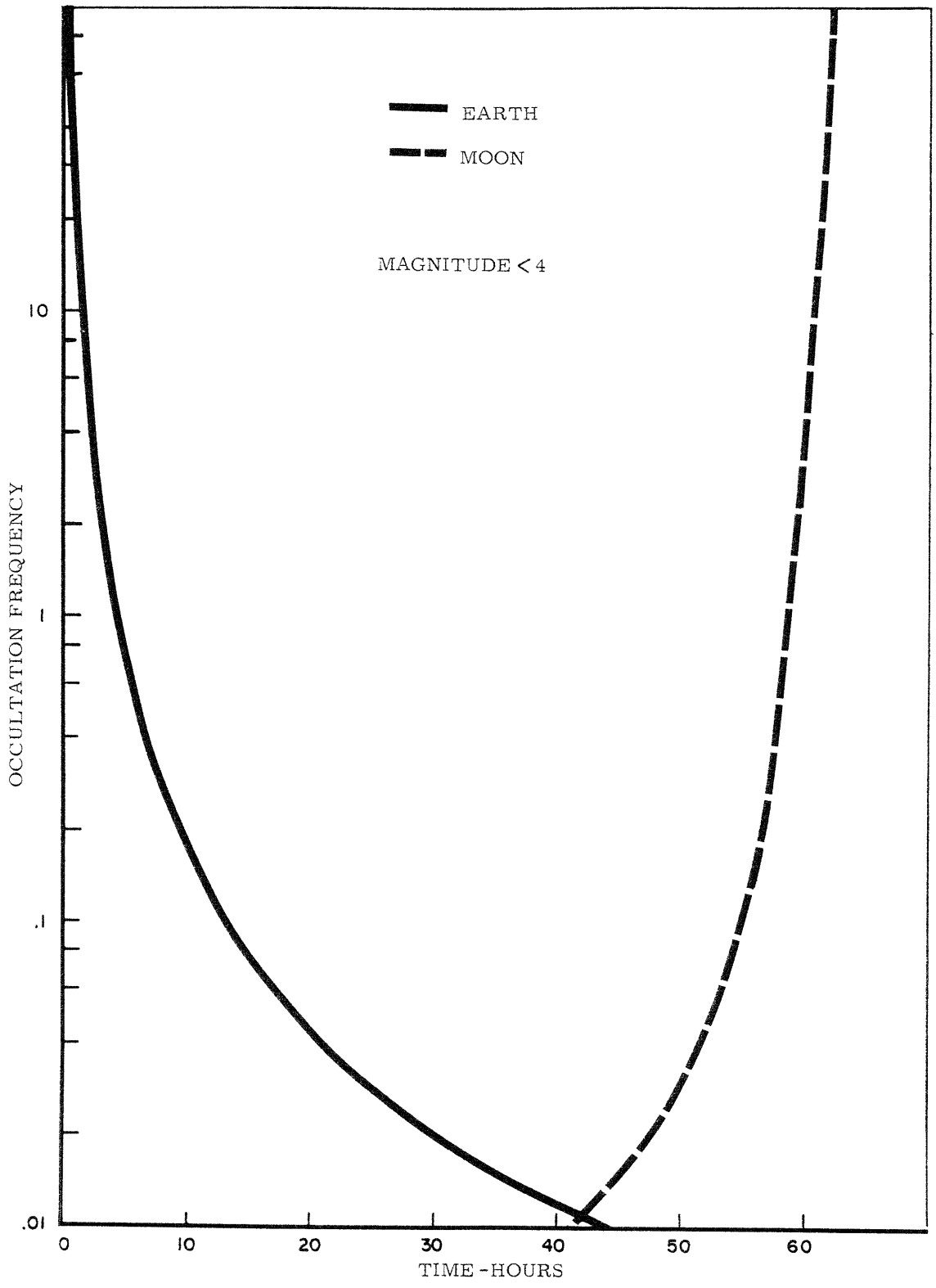
Fig. 4.1 Time history of occultation frequency

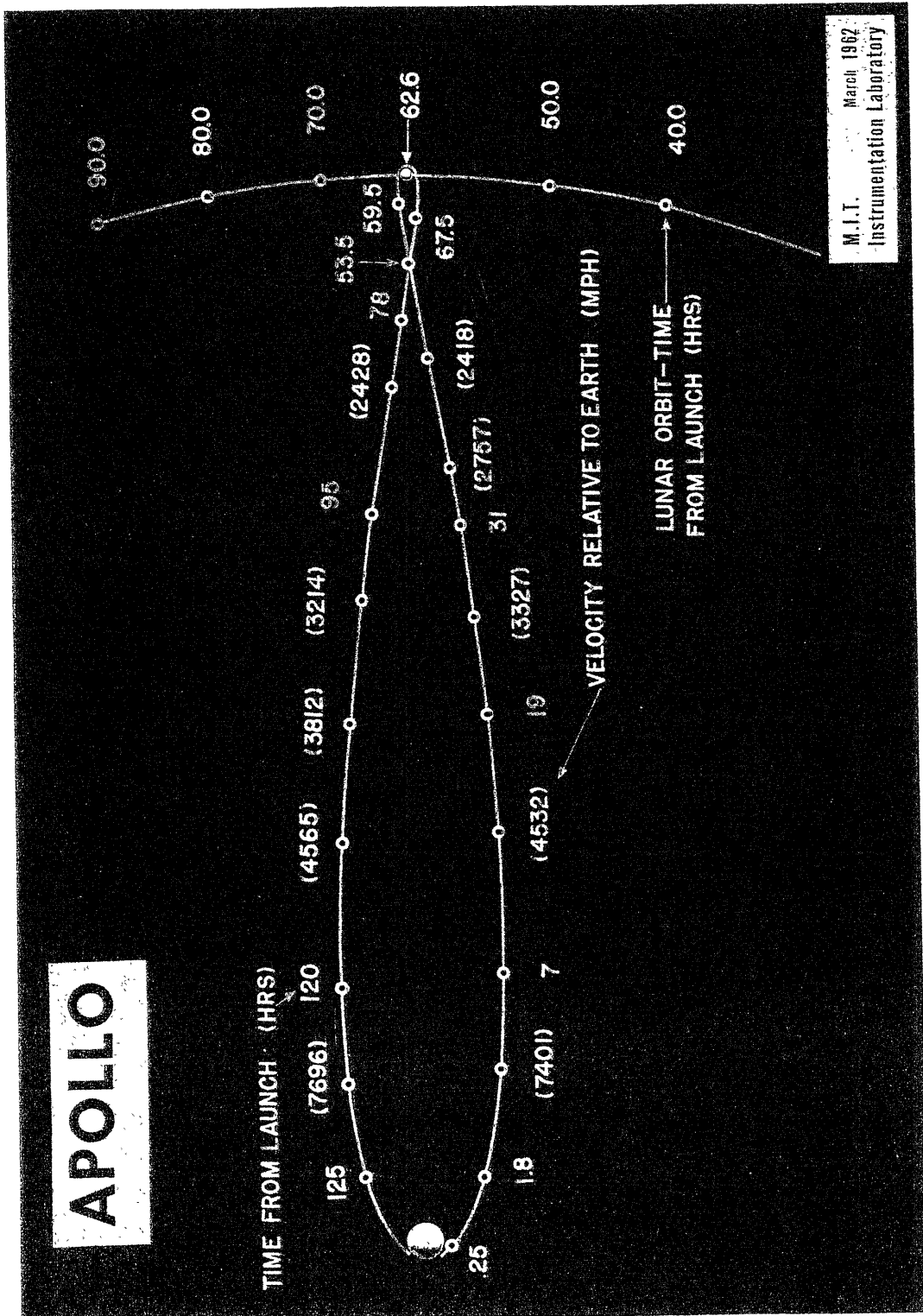Fig. 4.2 Time history of occultation frequency

Fig. 4.3   Circumlunar trajectory in Earth centered
non-rotating coordinates

approaches zero as would be expected. The corresponding
effect on occultations by the moon is noted during the
initial portion of the trajectory.

Fig. 4.2 would show the same trends as described in
the preceding paragraph if the ordinate were extended to
include smaller values of frequency. The maximum
occultation frequencies for stars of magnitude less than
four are 339 and 471 occultations per hour for the earth
and moon respectively.

4.5 The Number of Occultation Measurements Along the Trajectory

Fig. 4.4 is a plot vs. time of the occultations that
were measured during two simulated voyages. In one case
stars of magnitude less than four were considered and
in the other case stars of magnitude less than six were
considered. In both cases measurements of occultations
by the earth and by the moon are shown separately.

One of the principal disadvantages of star occultation
measurements is illustrated in Fig. 4.4. Occultations
occur so frequencly during the initial and moon approach
phases of the voyage that it would only be practical to
measure a fraction of the occultations that occur.
However, during a considerable portion of the voyage,
when the spacecraft is far from both bodies, the
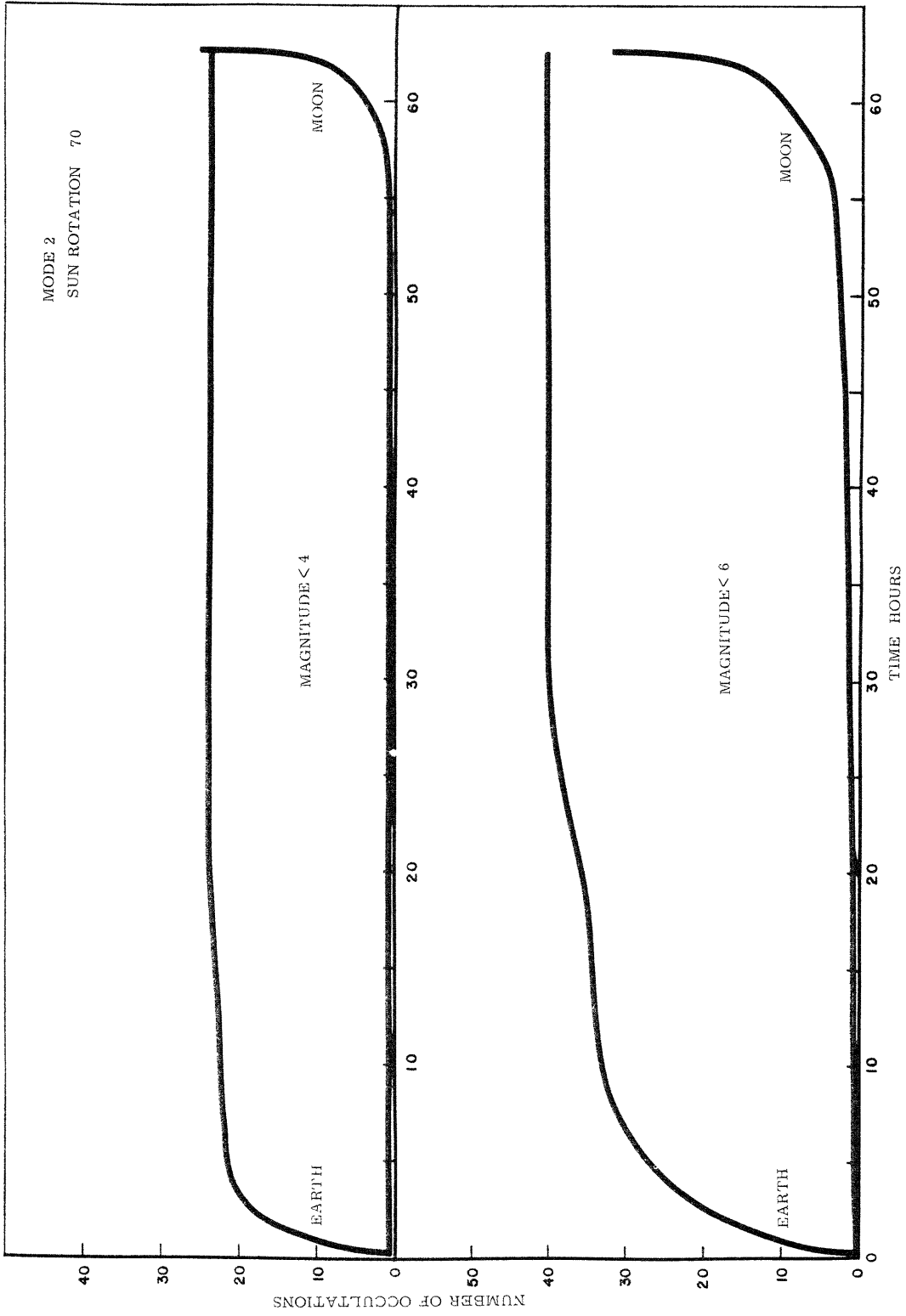
-66-

Fig. 4.4 Time history of occultations

probability that an occultation will occur is negligibly
small unless stars of magnitudes considerably larger
than six are considered.

4.6 Tabulation of Results

The results obtained from computer simulations of
the navigation modes and variations thereto described in
Section 4.3 are presented in Tables 4.2 and 4.3. The
results in Table 4.2 were obtained using a sun rotation
of 70 degrees. The applicable value of sun rotation is
specified in Fig. 4.3.

The authors will not attempt to discuss the implica-
tions of all the data presented in Tables 4.2 and 4.3.
Rather, several trends will be pointed out as examples
of the correlations that can be established between the
various results. The first two runs in Table 4.2
involve the use of occultation measurements only. The
first run uses only stars of magnitude less than four,
whereas the second run uses stars of magnitude less
than six. The results show that roughly the same
navigational accuracy is obtained in each case but at
the expense of almost five times the total velocity
correction when stars of magnitude less than four
are used. This result would be expected since Fig. 4.4
shows that the period during which no occultations

SUN ROTATION 70°

	Number of Earth Occultations Measured	Number of Moon Occultations Measured	Number of Angle Measurements	Number of Velocity Corrections	Total Velocity Correction (mph)	Final Velocity Uncertainty (mph)	Final Position Uncertainty (miles)	Final Miss Distance (miles)
Occultations Only Magnitude < 4	24	25	N/A	3	220	3.48	1.80	7.40
Occultations Only Magnitude < 6	40	32	N/A	3	48.2	2.78	1.34	3.78
Occultations and Angle Measurements Magnitude < 4	16	25	32	4	50.7	2.27	1.13	3.03
Occultations and Angle Measurements Magnitude < 6	28	29	32	3	36.2	2.43	1.19	5.03
Occultations and Angle Measurements Magnitude < 9	Not Computed	Not Computed	32	4	29.0	2.05	1.01	3.42
Occultations Only Occulting Body: Moon Magnitude < 4	N/A	24	N/A	3	827	8.10	3.58	7.04
Occultations and Angle Measurements Occulting Body: Moon Magnitude < 4	N/A	25	32	4	49.4	2.26	1.12	4.16

Table 4.2 Navigation data

Magnitude < 4

	Rotation (degrees)	Number of Earth Occultations Measured	Number of Moon Occultations Measured	Number of Angle Measurements	Number of Velocity Corrections	Total Velocity Correction (mph)	Final Velocity Uncertainty (mph)	Final Position Uncertainty (miles)	Final Miss Distance (miles)
Angle Measurements Only	70	N/A	N/A	32	3	84.0	19.8	6.76	10.1
Occultations Only	70	24	25	N/A	3	220	3.48	1.80	7.40
Occultations and Angle Measurements	70	16	25	32	4	50.7	2.27	1.13	3.03
Occultations and Angle Measurements Reduced Variance	70	16	24	32	5	54.5	.881	.402	.454
Occultations by Immersion Only Occulting Body: Moon	70	N/A	24	N/A	3	3760	11.7	4.79	6.84
Occultations by Immersion Only and Angle Measurements Occulting Body: Moon	70	N/A	25	32	3	84.0	4.33	2.04	10.1
Angle Measurements Only	250	N/A	N/A	32	3	165	3.17	1.35	10.2
Occultations Only	250	28	25	N/A	3	79.2	5.02	2.37	8.97
Occultations and Angle Measurements	250	17	22	32	4	68.5	1.99	.904	1.51
Occultations and Angle Measurements Reduced Variance	250	17	24	32	4	35.7	1.21	.564	2.03
Occultations by Immersion Only Occulting Body: Moon	250	N/A	26	N/A	2	194	92.3	44.5	70.9
Occultations by Immersion Only and Angle Measurements Occulting Body: Moon	250	N/A	23	32	4	86.4	2.29	1.01	1.95

Table 4.3 Navigation data

occur is considerably longer in the case where stars of magnitude less than four are used than it is when stars of magnitude less than six are used. Thus, with no measurements available, the errors build up to the point where a large velocity correction must be made relatively close to the moon.

From Table 4.3 it is interesting to compare, for both values of sun rotation, the run where navigation is accomplished by angle measurements alone, and the run where the angle measurements are supplimented by star occultation measurements of type NI+ by the moon. In both cases the addition of occultation measurements improves the results, but it is interesting to note that the same parameters are not improved in both cases. When the value of sun rotation is 70 degrees, the total velocity correction and final miss distance are unaffected while the final velocity and position uncertainties are improved substantially. When the value of sun rotation is 250 degrees the addition of occultation measurements reduces the total velocity correction by a factor of two and the final miss distance by a factor of five while the final position uncertainty and the final velocity uncertainty show little change.

Table 4.3 also shows the results of the simulations made with a reduced value of variance as described in Section 4.3 (1). In both cases the mode 3 results show a marked improvement over the mode 1 results. These results emphasize the need for accurately determining the values of the parameters that contribute to the variance.

4.7 Position Uncertainty

In addition to the end results of the various navigation modes presented in Section 4.6 it is informative to look at the time histories of the various navigation modes. In order to do this, a representative parameter must be selected. The authors chose U_p, the root mean squared position uncertainty at the destination if no more observations were made, for this purpose.

Fig. 4.5 shows the effect on this time history of changing the magnitude of stars used when the navigation is based on occultations alone. A large negative slope is desirable and is indicative of a large number of observations. In this case the large negative slope exists while the spacecraft is near the earth and again when it approaches the moon. The discontinuities following a portion of curve with a near zero slope correspond to the first occultation that occurs following
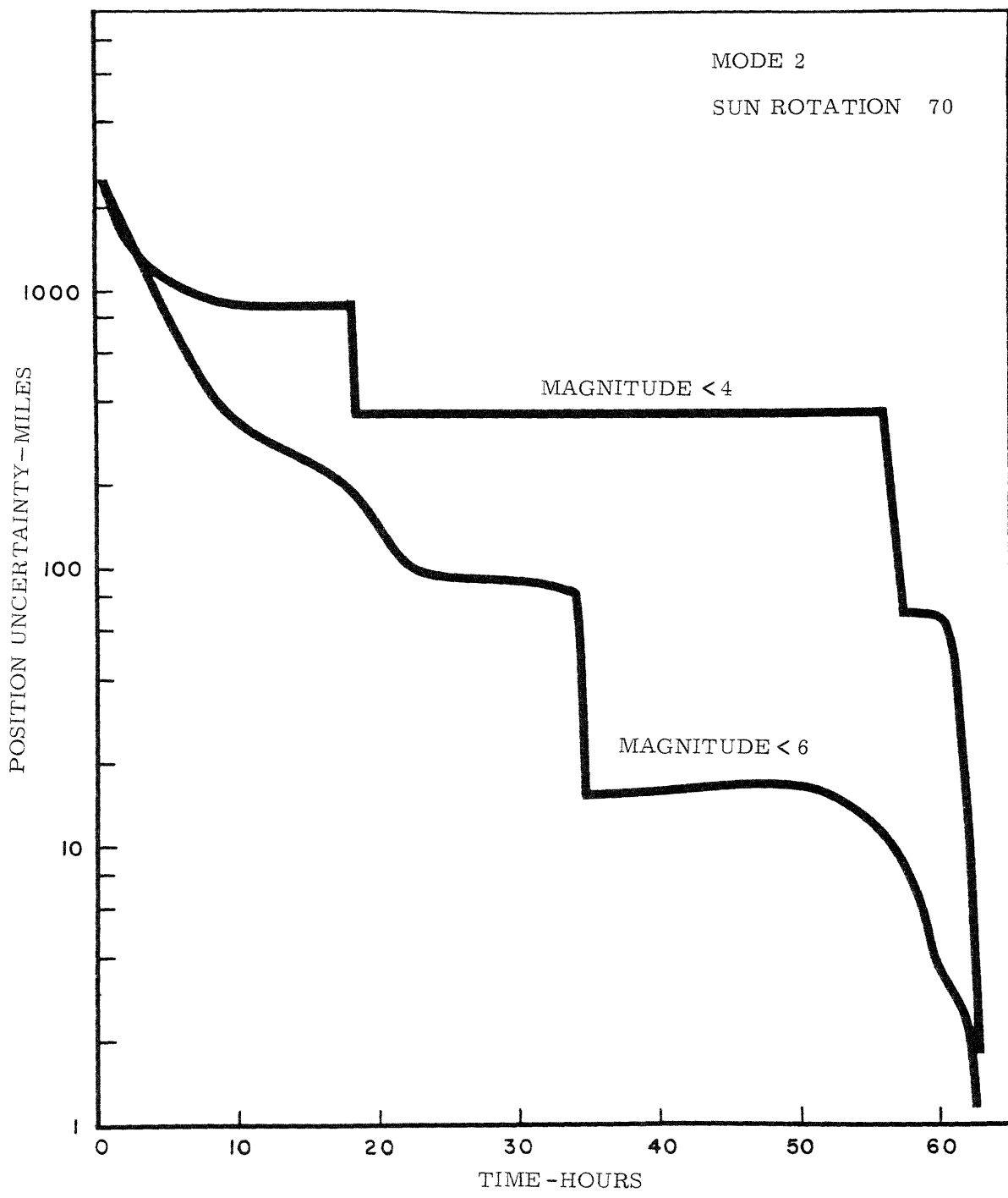
Fig. 4.5 Time history of position uncertainty

a period during which no measurements were available.
The discontinuity in the magnitude less than six curve at
34 hours can be traced to an early occultation by the
moon that is shown to occur in Fig. 4.4. The other
discontinuities can be traced in a similar manner.

With the exception of Fig. 4.5 all graphs of
position uncertainty vs. time are for stars of magnitude
less than four. This value was chosen as a compromise
between a manageable number of stars and the quantity
of stars necessary to provide a reasonable number of
occultations. There are approximately 500 stars in
this category.

Fig. 4.6 shows the time history of U_p for naviga-
tion modes 1, 2 and 3 with a sun rotation of 70 degrees.
This is the case where most of the moon as seen from the
approaching spacecraft is non-illuminated. Since this
condition is favorable for occultation measurements
and unfavorable for angle measurements, the improvement
in U_p shown in Fig. 4.6 when occultation measurements
are used in conjunction with angle measurements is as
would be expected.

The results shown in Fig. 4.7 are obtained in the
same manner as those shown in Fig. 4.6 with the
exception that the value of sun rotation is changed to
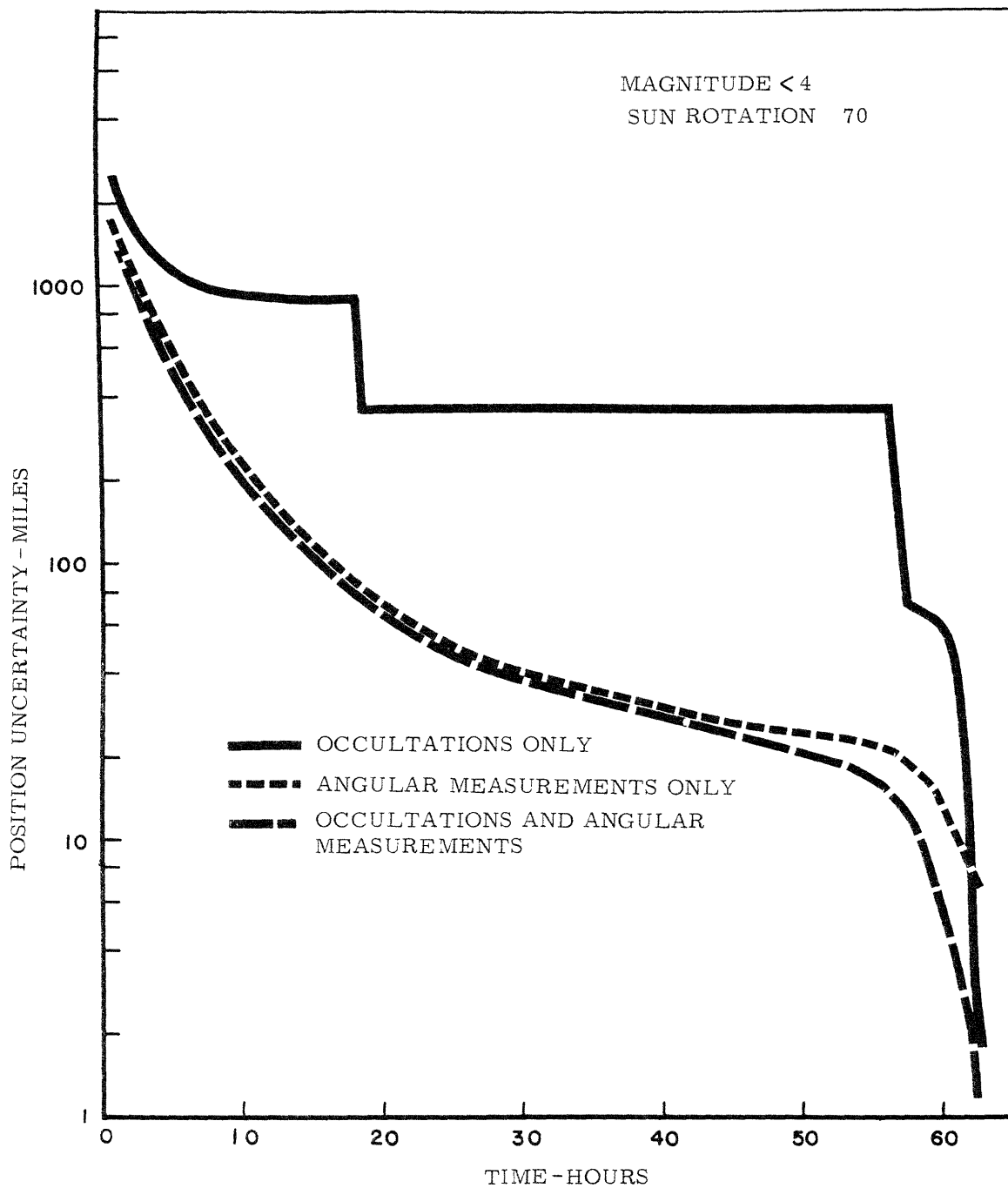250 degrees. This is the condition most favorable to angle

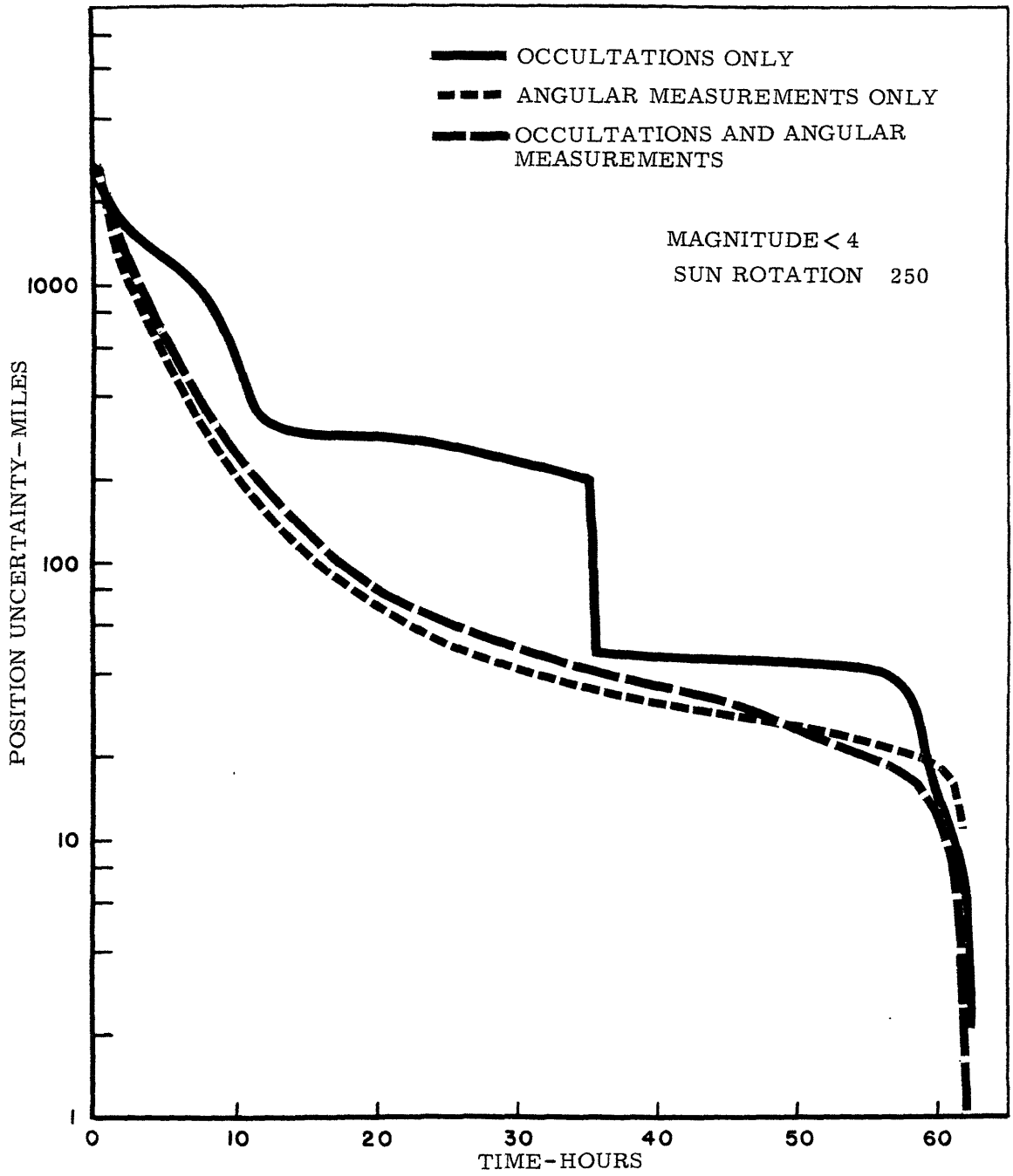Fig. 4.6 Time history of position uncertainty

Fig. 4.7 Time history of position uncertainty

measurements and least favorable to occultation measurements. The results here are also as would be expected. The addition of occultation measurements does not improve the time history of U_p to a great extent.

It should be pointed out at this point that the extreme decrease in U_p that occurs, starting at approximately 60 hours, is a somewhat unrealistic result of the computer simulation used. As was stated in Chapter 3 the program was written so that a measurement would be made at each decision point at which one or more occultations occur. Since the last three decision points are 1.2 minutes apart it is clear that observations could not be made as frequently on a real mission as they were during the final portion of this simulation. Thus, the mode 2 results in Fig. 4.6 are somewhat optimistic. By a careful analysis of Tables 4.2 and 4.3 this weakness in the simulation can be compensated for to some extent. In most cases a velocity correction was not made during this portion of the simulation so that the values of "total velocity correction" and "final miss distance" are not affected by this discrepancy.

Since the effect of earth occultation measurements is slight due to the large variance associated with them, two runs were made using only occultations by the moon. The results of these runs are shown in Fig. 4.8.
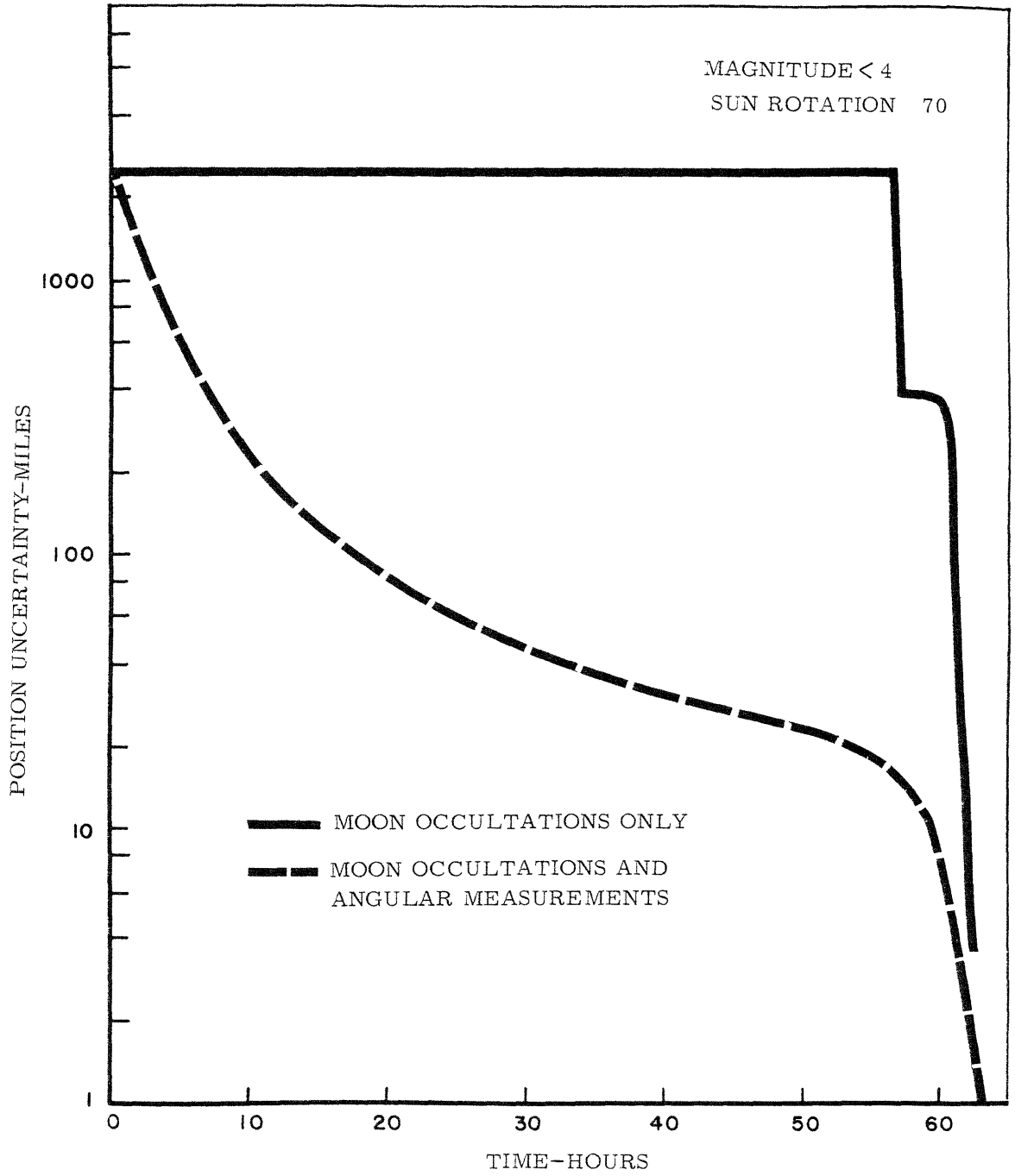
Fig. 4.8 Time history of position uncertainty

The variation to modes 2 and 3 described in Section 4.3 (2) resulted in the curves shown in Figs. 4.9 and 4.10. By using only NI+ occultations the number of measurements was reduced to an amount that might realistically be made. The number of measurements made is listed in Table 4.3.

4.8 Occultations of the 40 Brightest Stars

Since the results of the computer simulations indicated that occultation measurements would increase navigational accuracy and reduce the total velocity correction required, the authors wrote a program to determined how many actual occultations involving the 40 brightest stars could be observed by an astronaut aboard a spacecraft traveling along the first half of the circumlunar trajectory shown in Fig. 4.3. The results of this program appear in Table. 4.4.
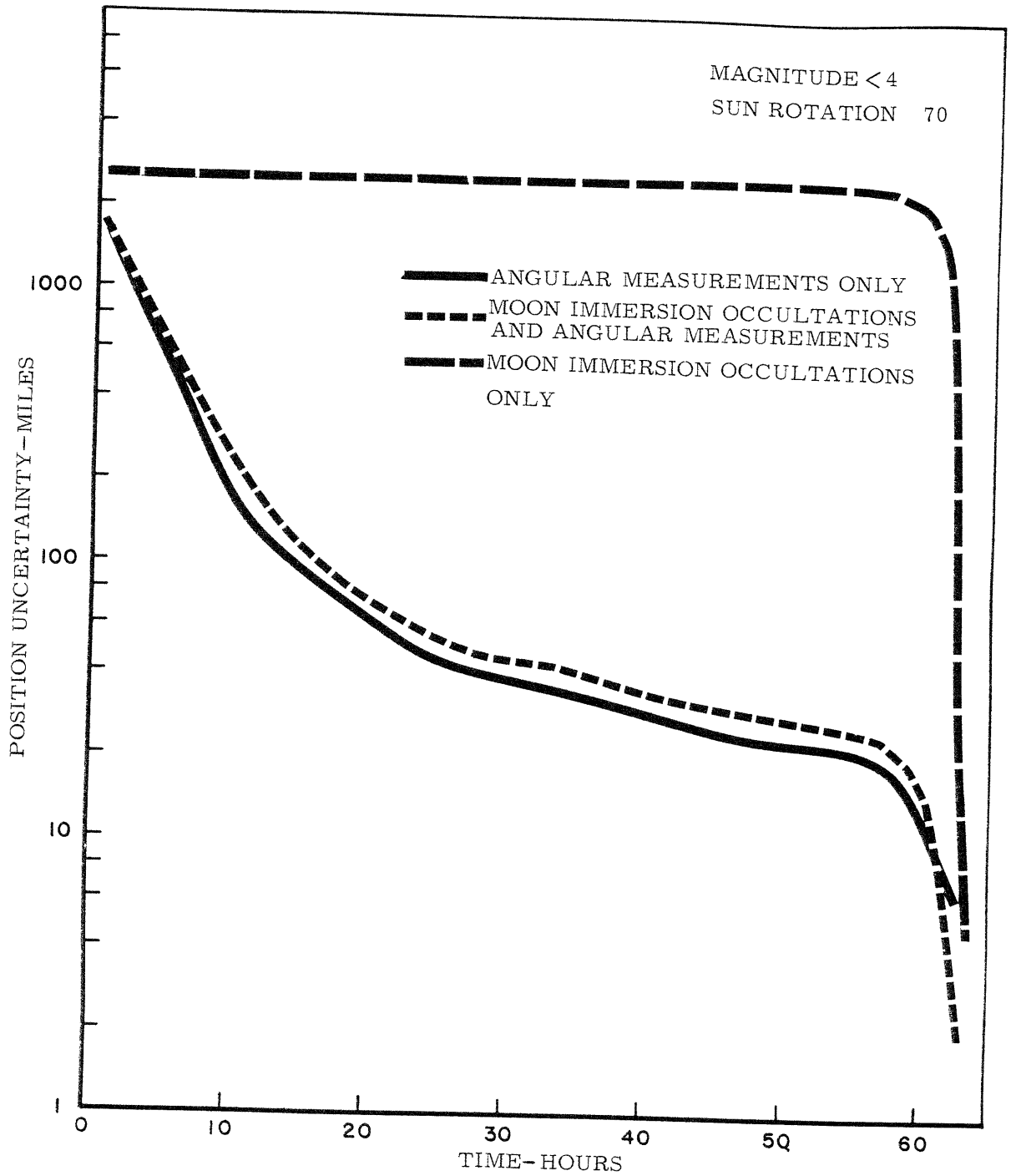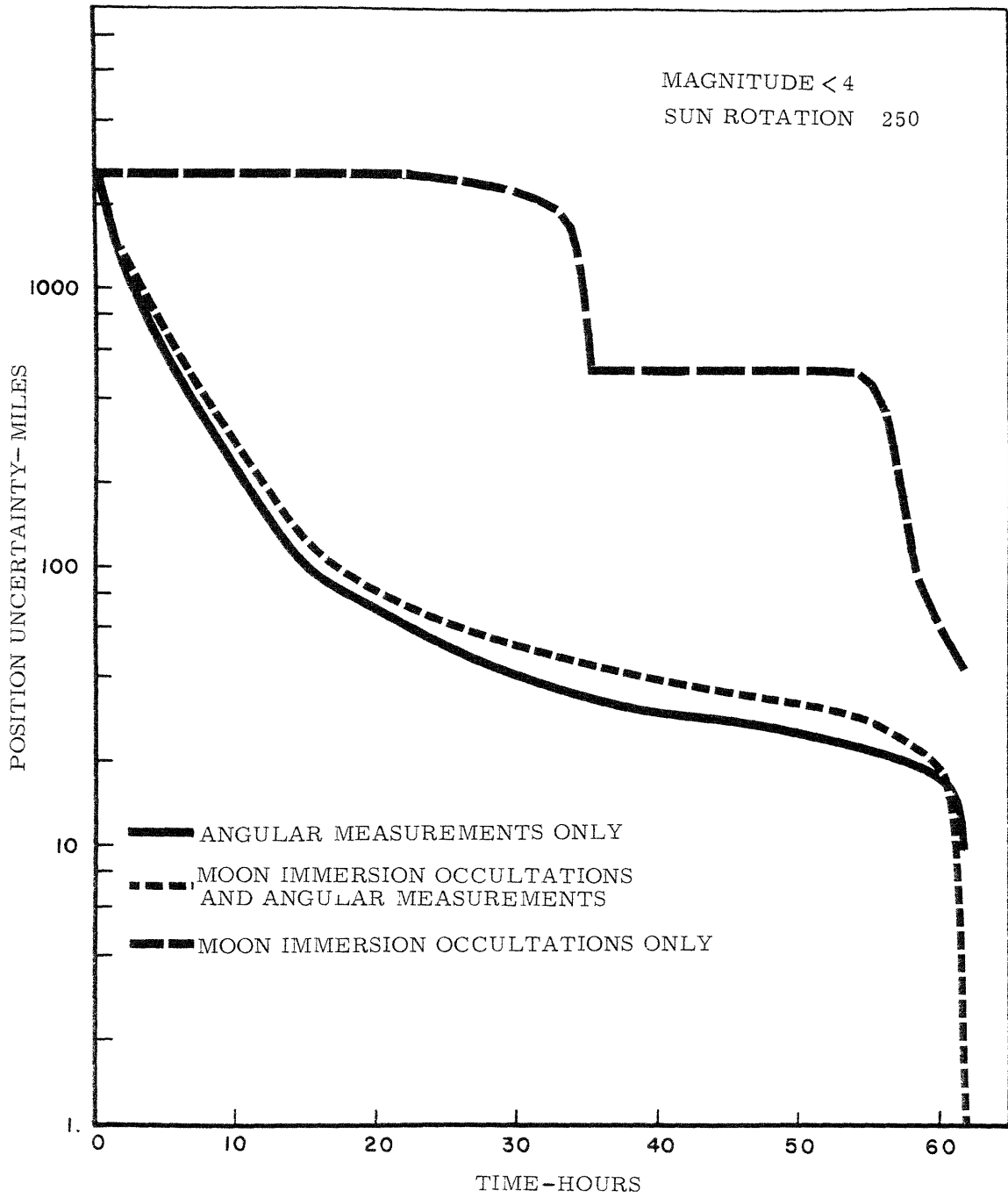
Fig. 4.9 Time history of position uncertainty

Fig. 4.10 Time history of position uncertainty

TABLE 4.4

OCCULTATIONS OF THE 40 BRIGHTEST STARS

Time (Approx)	Occulting Body	Immersion	Emersion
.30	earth		498*
.30	earth		380*
.70	earth	498	
.75	earth		498
2.20	moon	509	
3.00	moon	526	
3.40	moon	483	
24.00	moon	417	
62.38	moon		417
62.42	moon		483
62.44	moon		509
62.52	moon		526

380 - Regulus	498 - Spica
417 - Dubhe	509 - η Ursae Majoris
483 - ε Ursae Majoris	526 - Arcturus

*behind the earth at the beginning of the trajectory

CHAPTER 5

CONCLUSIONS

The simulations of various circumlunar navigation
techniques which were made during the course of this study
show that the inclusion of occultation measurements tends
to improve navigational accuracy and reduce the total
velocity correction required.

The accuracy with which occultations by the earth
can be observed was not accurately established. Therefore
more emphasis was placed on studying the effect of lunar
occultation measurements.

The value of utilizing occultation measurements in
addition to angle measurements is heavily dependent on
two factors: (1) the number of occultations that occur;
and (2) the accuracy with which occultations can be measured.
The number of occultations that occur is obviously
dependent on the magnitude of the stars considered.
There are several practical limits on the number of stars
that can be considered. The astronaut must identify each
star on which a measurement is based. As more stars are
considered this would become increasingly difficult. In
addition, data must be available on each star considered.

-83-

This too, would provide a limit on the number of stars that can be considered. The values used in this study for the variance associated with a lunar occultation were chosen conservatively. It was shown that a reduction in the parameters that determine the value of variance for an occultation results in a marked improvement in the quality of the navigation obtained.

The results obtained in this study indicate that angle measurements and occultation measurements might best be used in a complementary fashion, taking advantage of the favorable aspects of both types of measurements.

Since the initial occultation measurements are not very accurate due to the large variance associated with earth occultation measurements and since occultation measurements are practically non-existent during the mid-portion of the trajectory, angle measurements alone might be used until approximately 55 hours have passed. At this time the navigator would switch over to occultation measurements entirely, since it is reasonable to assume that more occultation measurements than angle measurements can be made in a given amount of time. The quality of both types of measurements is comparable in this region. Thus, by virtue of the greator quantity of measurements made, this scheme should improve the

navigational accuracy.

Since this study was based on a statistical star background rather than an actual star field, no final conclusions concerning the advisability of using star occultation measurements can be reached. However, based on the results of this study the authors feel that further investigation using actual star data would be appropriate.

REFERENCES

1. Battin, R.H., "A Statistical Optimizing Navigation Procedure for Space Flight", M.I.T. Instrumentation Laboratory Report, R-341, September 1961.

2. Laning, J.H. Jr., "Statistical Study of Occultations for Circumlunar Orbits", March 1961, (unpublished).

3. Battin, R.H., and Miller, J.S., "Circumlunar Trajectory Calculations", M.I.T. Instrumentation Laboratory Report, R-353, April 1962.

4. Allen, C.W., Astrophysical Quantities, The Athlone Press, 1955.

5. Baldwin, R.B., The Face of the Moon, University of Chicago Press, 1959.